NUWC-NPT Technical Report 10,797
23 January 1995

Molecular Modeling of PMN Ceramics

George J. Kavarnos
Submarine Sonar Department

Naval Undersea Warfare Center Division
Newport, Rhode Island

PREFACE

The work described in this report was sponsored by the Naval Undersea Warfare Center's Independent Research (IR) Program, as Project No. A10016 entitled "Molecular Modeling of New Transducer Materials." The IR Program is funded by the Office of Naval Research; the NUWC program manager is Dr. Kenneth M. Lima (Code 102).

The technical reviewer for this report was Dr. Harold Robinson (Code 3111).

The author acknowledges with deep gratitude the continued support and encouragement of Dr. Kenneth Lima (Code 102) and the scientific expertise of Jan Lindberg (Code 213) and James Powers (Code 2131).

Reviewed and Approved: 23 January 1995

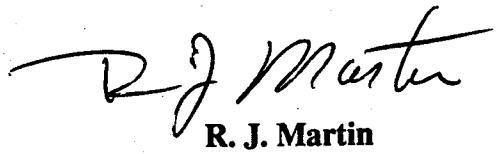

R. J. Martin
Head, Submarine Sonar Department

REPORT DOCUMENTATION PAGE

Form Approved
OMB No. 0704-0188

1. AGENCY USE ONLY (Leave Blank)	2. REPORT DATE	3. REPORT TYPE AND DATES COVERED
	23 January 1995	Final

4. TITLE AND SUBTITLE

Molecular Modeling of PMN Ceramics

5. FUNDING NUMBERS

PR A10016

6. AUTHOR(S)

George J. Kavarnos

7. PERFORMING ORGANIZATION NAME(S) AND ADDRESS(ES)

Naval Undersea Warfare Center Detachment
39 Smith Street
New London, Connecticut 06320-5594

8. PERFORMING ORGANIZATION REPORT NUMBER

TR 10,797

9. SPONSORING/MONITORING AGENCY NAME(S) AND ADDRESS(ES)

Naval Undersea Warfare Center Division
1176 Howell Street
Newport, Rhode Island 02841-5594

10. SPONSORING/MONITORING AGENCY REPORT NUMBER

11. SUPPLEMENTARY NOTES

12a. DISTRIBUTION/AVAILABILITY STATEMENT

Approved for public release; distribution is unlimited.

12b. DISTRIBUTION CODE

13. ABSTRACT (Maximum 200 words)

Extended Hückel theory was used to analyze the orbital interactions in $PbNbO_3^{1+}$ and $LaNbO_3^{2+}$ model structures representative of lead magnesium niobate (PMN)ceramic. These structures were chosen to determine the orbital effects, if any, that an A-site substitutional such as Pb^{2+} has on bond stability in the crystal lattice structure. It was determined that the A-site ion does not directly influence bonding between the A-site ion and atoms in the neighboring crystal lattice but does change the position of the Fermi level, which in $PbNbO_3^{1+}$ is −10.1 eV and in $LaNbO_3^{2+}$ is −14.5 eV. In $PbNbO_3^{1+}$, the Fermi level is so positioned that the bonds linking Nb and O are destabilized. In contrast, there is no antibonding character in $LaNbO_3^{2+}$. The shifting of the Fermi level as a function of the A-site ion is used to rationalize the experimental observation that pure PMN does not coarsen or undergo additional crystallization during annealing, but La-substituted PMN does in fact favor ordering of the crystal structure.

14. SUBJECT TERMS
Molecular Modeling
Piezoelectric Polymers
Piezoelectric Properties

15. NUMBER OF PAGES
35

16. PRICE CODE

17. SECURITY CLASSIFICATION OF REPORT	18. SECURITY CLASSIFICATION OF THIS PAGE	19. SECURITY CLASSIFICATION OF ABSTRACT	20. LIMITATION OF ABSTRACT
Unclassified	Unclassified	Unclassified	SAR

TABLE OF CONTENTS

LIST OF ILLUSTRATIONS

LIST OF TABLES

Reverse Blank

MOLECULAR MODELING OF PMN CERAMICS

INTRODUCTION

Electrostrictive materials are capable of delivering huge strains when stressed by electric fields. One of the leading candidate electrostrictive materials is lead magnesium niobate (PMN), which is currently attracting much interest in the transducer community. The strains that PMN can achieve on application of high field are greater than the strains in normal piezoelectric ceramics such as lead zirconate titanate (0.1%). It is also noteworthy that PMN does not have to be poled as does conventional piezoelectric ceramic. It belongs to a class of relaxor ferroelectrics which displays a diffuse phase transformation. However, in contrast to normal ceramics that are capable of undergoing a phase transformation into a long-range ferroelectric state, a relaxor such as PMN displays micropolar regions about 50 Å in diameter. To rationalize the pronounced electrostrictive effect in PMN materials, Cross[1] has examined the role of compositional heterogeneity of fluctuations in $A(B_1B_2)O_3$ relaxor perovskites where A, B_1 and B_2 are cations (in the case of PMN, A is lead, B_1 is magnesium, and B_2 is niobium). In the Cross model, compositional variations in B-site ordering lead to differences in local and global symmetry. Since local symmetry is lower than the global symmetry, polar orientation states of each microregion are not identical, and the energies of each polar state are no longer degenerate. This leads to the creation of *dynamically disordered polarization states.* The ramifications of dynamically disordered polarization are far reaching, for this model implies that coupled dipoles will oscillate and respond to an applied electric field leading to large and diffuse permittivity and large electrostrictive strains.

Ordering of the B-site atoms is in part governed by the ionic radii and charge of the B cations; thus, the tendency to order is due to elastic forces and electrostatic interactions. Using transmission electron microscopy (TEM), Viehland[2,3] has identified ordered regions in $Pb(Mg_{1/3}Nb_{2/3})O_3$ compositions where the B-site ion ratio is 1:2. During annealing, these regions do not coarsen. The inability of the micropolar regions to grow in size during annealing is due to microstructural chemical effects that prevent the development of the normal long-range order. However, in a material such as $Pb(Sc_{1/2}Ta_{1/2})O_3$, which has an ordered B-site ratio of 1:1, the ordered domains coarsen during annealing.[4] This observation led Viehland and others to suggest that the clustered regions in PMN are characterized by a nonstoichiometric 1:1 ordering of Mg and Nb.[5,6] With a 1:1 ratio of B-site ions, the ordered region is electrically nonneutral. The development of the ordered regions is then dictated by opposing stabilizing long-range and destabilizing short-range electrostatic interactions. Viehland has suggested that the size of the ordered domains is a result of charge variations due to mixed B-site occupancy. According to this view, ordered domain size and subsequently the electromechanical properties can be manipulated by creating defect structures such as can be achieved by the

introduction of oxygen-deficient sites. Substitutions for A-site atoms can bring about changes in annealing and ordering behavior. For example, substitution of La^{3+} for Pb^{2+} forces ordering of Nb^{5+} and Mg^{2+}.[7] However, substitution of Ba^{2+} or Sr^{2+} for Pb^{2+} significantly reduces the relaxor response.[8] It is clear that the A-site ion must influence the size of the ordered domains and therefore the electromechanical response. Because La^{3+} is aliovalent, its substitution into the A-site may be accompanied by the formation of oxygen vacancies to compensate for the positive charge.

Another complication in the PMN puzzle has to do with the possibility of structural nonuniformities in the ordered 1:1 microregion. Experiments employing atomic resolution transmission electron microscopy have demonstrated the existence of strong nonuniform polarized transverse strain waves in the ordered regions.[9] One hypothesis for this observation is that the nonuniform distortions are due to the presence of an "embryonic" $Pb_2Nb_2O_7$ pyrochlore phase with the perovskite phase. The presence of this inhomogeneity may be responsible for the development of local polarization and the absence of a long-range ferroelectric phase.

Quite germane to PMN is an alternative atomistic model. Thomas proposed that indirect <110> coupling dominates in PMN and influences B-site ordering.[3] In the Thomas model, the temperature at which an individual octahedron becomes decoupled from its neighboring octahedron gives rise to a Curie point distribution function which can explain the diffuseness of the ferroelectric-paraelectric phase transitions in PMN ceramics. A ferroelectrically active microregion consisting of active NbO_6 octahedra is surrounded by inactive MgO_6 octahedra. Between the NbO_6 cluster and MgO_6 surroundings there exists a dynamic wall rich in MgO_6. The NbO_6 octahedra within the wall are coordinated (coupled) with fewer NbO_6 so that they undergo a ferroelectric-paraelectric transition and decoupling at a lower temperature than the coupled NbO_6 within the cluster. As decoupling within the wall proceeds, more NbO_6 octahedra become uncoupled and the "wall" propagates towards the center of the microregion. All of this can give rise to the diffuse phase transition characteristic of PMN ceramics.

It is therefore abundantly clear that to manipulate the electromechanical response of PMN, attention must be given to compositional control of PMN. Compositional modification can be achieved by altering the A- or B-site atom or by oxygen-deficient ordering. These modifications can lead to optimization of the electromechanical properties of PMN. Current research has been directed to material development of PMN compositions with special emphasis on improved performance such as increased induced strain, decreased strain hysteresis, increased coupling, and reduced temperature dependence of strain and polarization behavior.[10, 11]

The objective of the present research was to examine the effects of A-site substitutionals on the bonding and stability of the ordered regions, from the

perspective of semiempirical quantum mechanics. We propose that ordering behavior in PMN might be related to interactions between the orbitals of the A-site atom with the orbitals involved in bonding of the B-site atoms and oxygen. Because there has been no analysis of orbital interactions in PMN ceramics, it may be fruitful to examine how orbital overlap or bonding between Nb and O and between Mg and O is related to the nature of the A-site atoms. There are several ways to depict these orbital interactions. In a NbO_6 perovskite, niobium is coordinated in the <100> direction in an octahedral environment by six oxygen atoms. Niobium-oxygen bonding can involve the interaction of 2s and 2p orbitals in oxygen and the e_g ($4d_{z^2}$ and $4d_{x^2-y^2}$) orbitals in niobium (figure 1). The remaining niobium t_{2g} ($4d_{xy}$, $4d_{xz}$, and $4d_{yz}$) orbitals might be expected to interact with the 2p oxygen orbitals to generate π-bonding (figure 1). We are hypothesizing that the nature of the A-site atom influences the local bonding in the PMN crystal lattice, and this is brought about by changing the electron count and position of the Fermi level. If indeed the stability of the PMN microregions is related to bonding, can a predictive model be formulated to show how substitution of other atoms on the A-site is related to the size and character of the microregions necessary for electrostriction?

This proposal represents an effort to explain the electrostrictive phenomenon in PMN ceramics within the framework of molecular orbital theory, which has been used by chemists to successfully predict and study structure-property relationships of numerous solid-state materials. In effect, the research suggested here will bring together the language of chemistry and physics to study relaxor properties.[12,13,14,15] An atomistic approach to the composition variation in PMN and the implications of composition in electrostriction may ultimately result in a predictive model. The work described here is based on a previous study of the effects of orbital interactions in ordered-defect rock-salt structures, where it was demonstrated that metal-metal and metal-oxide bonding helps to stabilize these structures.[16] The approach in the present study was to determine the role of band structures, density of states, and orbital overlap populations on bond stability in model perovskite structures representative of PMN.

THEORY

An understanding of orbital interactions in solid materials can lead to an improved understanding of material properties such as bond stability. Bonding in crystal structures can be formulated in the language of band orbitals. The theory is described in the next section.

BAND ORBITALS

Orbital interactions in several crystal models of PMN were studied using extended Hückel (EH) molecular orbital theory. When applied to solid-state materials, the EH approach gives a band structure calculation, which can be used to analyze bonding. When applied to a one-dimensional lattice containing one atom per unit cell, the atomic orbital (φ) can be represented by a Bloch orbital shown as follows:

$$\phi_\mu(k)=N^{-1/2}\sum_n \exp(ikna)\chi_\mu, \tag{1}$$

where χ_μ is an atomic orbital on the atom in the n-th unit cell, N is the number of unit cells in the solid, k is a wavevector along the one-dimensional direction, and a is the lattice dimension of the one-dimensional cell. Values of the wavevector are defined by

$$-\pi/a \le k \le \pi/a. \tag{2}$$

Crystal orbitals are linear combinations of Bloch orbitals:

$$\Psi_i(k)=\sum_{\mu=1}^{M} c_{\mu i}(k)\phi_\mu(k). \tag{3}$$

The eigenvalues of the Hamiltonian, H, of equation (3) represent the energies, $E_i(k)$, of the crystal orbitals:

$$H\Psi_i(k)=E_i(k)\Psi_i(k). \tag{4}$$

Minimizing the energy with respect to the coefficients gives a secular determinant:

$$H_{\mu\nu}(k)-E_i(k)S_{\mu\nu}(k)=0, \tag{5}$$

where

$$H_{\mu\nu}(k)=\langle\phi_\mu(k)|H|\phi_\nu(k)\rangle \tag{6}$$

and

$$S_{\mu\nu}(k) = \langle \phi_\mu(k) | \phi_\nu(k) \rangle. \quad (7)$$

Solution of equation (5) leads to

$$E(k) = \alpha + 2\beta \cos ka, \quad (8)$$

where α is the Coulomb integral and β the nearest neighbor resonance integral. For a series of overlapping orbitals, a plot of E(k) *vs.* k can be obtained. The width of the band, or the magnitude of interaction between the orbitals on neighboring atoms, is given by 4β. In other words, a chain of strongly interacting orbitals results in a large dispersion or large 4β.

The plot of E(k) *vs.* k, which is called a band structure diagram, allows one to analyze the electronic properties of solid-state materials. The range of k is called the first Brillouin zone, which can be constructed using the reciprocal crystal lattice. From the band structure, we can calculate the density of states (DOS), which represents the number of levels at a given energy. To calculate the bonding characteristics between two atoms in a solid-state material, the overlap population represents the overlap integrals summed over all orbitals of the two atoms. The overlap population weighted density of states is called the crystal orbital overlap population (COOP). The COOP describes the way the orbitals interact and allows one to determine the strength of bonding.

MODEL CRYSTALS

The crystal structure of PMN at room temperature is a cubic perovskite belonging to space group *Pm3m*. The lattice dimension is about 4.04 Å.[17,18] To study the effects of A-site substitution on Nb-O bonding along the <100> crystallographic directions, the models chosen for this study were $PbNbO_3^{1+}$ and $LaNbO_3^{2+}$. Figure 2 shows the unit cell crystal structure of $PbNbO_3^{1+}$. The structure of $LaNbO_3^{2+}$ is similar. These structures have Nb positioned at the corners (0, 0, 0) of a primitive cubic unit cell. The Nb is coordinated along the cell edges with oxygen atoms at the edge centers at (1/2, 0, 0; 0, 1/2, 0; 0, 0, 1/2). The A-site cation, Pb^{2+} or La^{3+}, is placed in the body-centered position at (1/2, 1/2, 1/2). The size of the $PbNbO_3^{1+}$ and $LaNbO_3^{2+}$ unit cell was set at 3.7 Å, which implies a bond length of 1.85 Å for Pb-O and La-O. This size was chosen to correct for the diffuseness of the atomic orbitals and to maximize orbital overlap.

The crystals were modeled as three-dimensional lattice systems with the **k** vector changing within a three-dimensional Brillouin zone. The points in the three-dimensional zone, which correspond to certain points of the cubic lattice as shown in figure 3, are Γ, M, X, and R.[19] The directions in reciprocal space in this cubic lattice are therefore Γ to M, M to X, X to R, and R to Γ. k-space meshes consisted of 40 k points. The Hückel parameters used in the molecular orbital calculations are listed in table 1.

RESULTS AND DISCUSSION

A preliminary study was first undertaken to obtain a qualitative orbital description of bonding in the model crystal structures. The electronic configurations of Nb, Pb, and La are listed in table 2. Niobium uses its 4d and 5s electrons to form σ-bonds and π-bonds with the 2s and 2p orbitals of surrounding oxygen atoms. To examine the nature of this bonding and how it changes along the Brillouin zone and affects the band structure, it is best to consider the interactions to form π-bonds in a simple one-dimensional repeating chain. Figure 4 shows the two band structures of a one-dimensional chain of alternating niobium and oxygen and the interactions between the oxygen $2p_z$ and niobium $4d_{xz}$ Bloch orbitals. At $k = 0$, the $2p_z$ and $4d_{xz}$ Bloch orbitals do not mix because of differences in symmetry. The $2p_z$ Bloch orbital is symmetric with respect to rotation about the z-axis, whereas the $4d_{xz}$ orbital is asymmetric. This implies that these orbitals should not interact at $k = 0$. However, at $k = \pi/2$, both orbitals are allowed to mix because of symmetry. As a result of orbital mixing, two new states are created, one characterized by strong orbital overlap and therefore at lower energy and the other having antibonding interactions. The direct consequence on changing the wavevector from Γ to X leads to a gradual lowering of the energy of the $2p_z$ Bloch orbital and a gradual increase in $4d_{xz}$. Similar arguments can be invoked for the more complex three-dimensional structures. Although the resulting band structures can be quite complicated, orbital interactions can be depicted as in the case of the simple one-dimensional repeating chain to gain an intuitive perception of orbital interactions. The number of bands in the structure is equivalent to the number of interacting orbitals. Some bands will be steep because of strong orbital overlap and others will be flat. The bands are influenced by both the symmetry and topology of the interacting orbitals. In general, more diffuse orbitals such as s and p give rise to strong dispersion; contracted orbitals such as d result in flat and dispersionless bands.

It is more instructive to analyze DOS and COOP plots rather than the complex, sphaghetti-like band structures. The DOS plots of $PbNbO_3^{1+}$, and $LaNbO_3^{2+}$ are illustrated in figures 5 and 6, respectively. The separate orbital contributions of the oxygen, A-site lead or lanthanum, and B-site niobium to each DOS are shown as dashed lines in figures 7 to 21. Consider first the DOS plots of $PbNbO_3^{1+}$. The

interactions between the 5p, 6s, and e_g ($4d_{z^2}$ and $4d_{x^2-y^2}$) orbitals of niobium with the 2p orbitals of oxygen contribute to σ- and π-bonding (figure 1). This is shown by the contributions to the overall DOS of the O 2p bands in figure 7 and of the Nb 5s, 5p, and e_g bands in figures 8 to 11. The formation of π-bonding can occur by overlap between the 5p and t_{2g} niobium orbitals and 2p oxygen orbitals. This is illustrated in figure 1, which shows the overlap between a d_{xz} niobium and a 2p oxygen orbital. Similar considerations apply to the bands in $LaNbO_3^{2+}$ (figures 12 to 16).

Now, let us consider the contributions of the A-site atomic orbitals to the DOS. For $PbNbO_3^{1+}$, the contributions of the 6s and 6p lead orbitals to the DOS are shown in figures 17 and 18. Here the 6s and 6p bands, which are well separated and at higher energies, make a small contribution to the density of the 2p oxygen and 5s and 5p niobium. The contributions of the lanthanum 6s, 6p, and t_{2g} orbitals are exemplified in figures 17 to 21. Again, we note small contributions to the lower energy bands. We conclude that A-site atoms do not bond with neighboring atoms in the crystal lattice.

So far, our analysis has revealed nothing unusual from the DOS plots. The orbital interactions to form σ- and π-bonds support our expectations. The nature of the A-site atom does not seem to influence these interactions. For a complete picture, however, we need a way to describe the bands as either bonding or antibonding. We can do this by calculating the overlap integrals between the niobium and oxygen summed over all orbitals in these atoms to give a COOP. Positive overlaps signify bonding; negative overlaps imply antibonding. As shown in figures 22 and 23, the COOP's of $PbNbO_3^{1+}$ and $LaNbO_3^{2+}$ are not identical. To appreciate this difference, we have specified the position of the Fermi level for both models. The Fermi level lies midway between the highest bonding and lowest antibonding orbitals. Its position is, therefore, determined by the number of electrons occupying the orbitals. The trivalent state of lanthanum has one electron less than the divalent state of lead. This suggests that the Fermi level should be lower when La^{3+} is substituted in the A-site. Indeed, calculations show that in $LaNbO_3^{2+}$, the Fermi energy lies at about -14.5 eV, whereas in $PbNbO_3^{1+}$ the Fermi level is -10.1 eV. It is particularly significant that near the Fermi level in $PbNbO_3^{1+}$ there is an antibonding Nb-O band partially occupied by electrons. This suggests that substitution of Pb^{2+} in the A-site may destabilize the bonding between niobium and oxygen giving rise to weaker bonds in the crystal structure. The magnitude of this destabilization is such that long-range ordering and crystallization may be more difficult when Pb^{2+} exclusively occupies the A-site. Substitution of La^{3+} in the A-site, however, is predicted to favor bonding along the <100> crystallographic directions and, therefore, ordering and crystallization.

The calculations in this investigation must be regarded as tentative. More work is needed to test this theory on various models and establish trends. To

examine the consequences of bonding and orbital interactions in PMN, it is proposed to extend this preliminary work to superlattice structures of PMN, to examine the orbital and electronic effects of substitutions of Ba^{2+}, Sr^{2+}, and other cations in the A-site, and to correlate these effects with the position of the Fermi level.

CONCLUSIONS AND RECOMMENDATIONS

The original objective of this work was to demonstrate that molecular modeling is a practical tool for the study of ceramics used in Navy underwater transducers. Given the formidable complexity of the ceramic PMN, there is strong reason to develop structure/property relationships, which may lead to a judicious selection of PMN compositions and processing conditions. We chose to study the effect of an A-site substitutional, lanthanum, on the annealing properties of PMN, a candidate electrostrictive ceramic for high power sonar projection. To approach this problem, we have chosen a semiquantum mechanical approach called extended Hückel theory where band structures, density of states, and crystal overlap populations can be calculated. These calculations can be used to explain certain properties of the ceramic. In the present work, we propose a tentative explanation for the lack of ordering in PMN ceramic when lead exclusively occupies the A-site in the crystal lattice. In contrast, when lanthanum is substituted for lead, there is an enhancement in bond stability and a tendency for long-range ordering and annealing. This markedly changes the electrostrictive properties of the ceramic.

Of course, this is only part of the story. We have not considered the potential role of oxygen defects in La-substituted PMN, the effects of other substitutionals, and the nature of the electrostatic effects arising because of charge imbalances between the ordered and nonordered regions. These are all issues which will have to undergo scrutiny. In the meantime, we are extending this work to develop a more complete picture of the role of orbital interactions in ceramics for transducers.

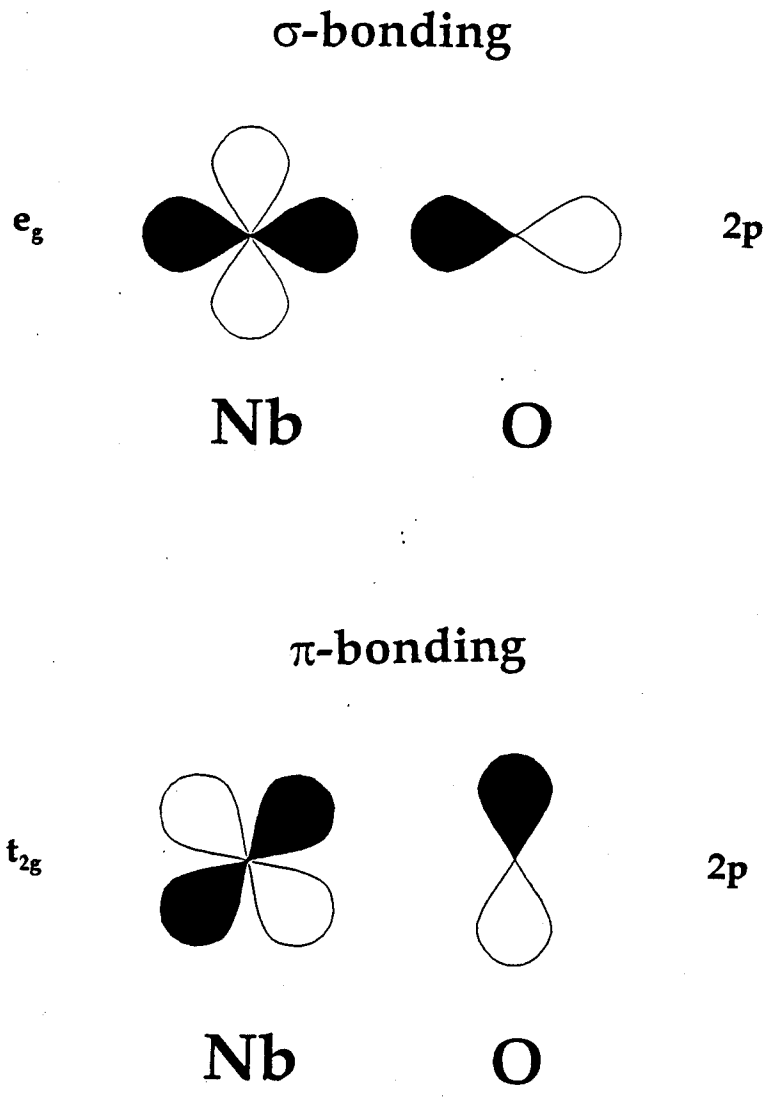

Figure 1. Orbital Interactions in PMN Ceramics

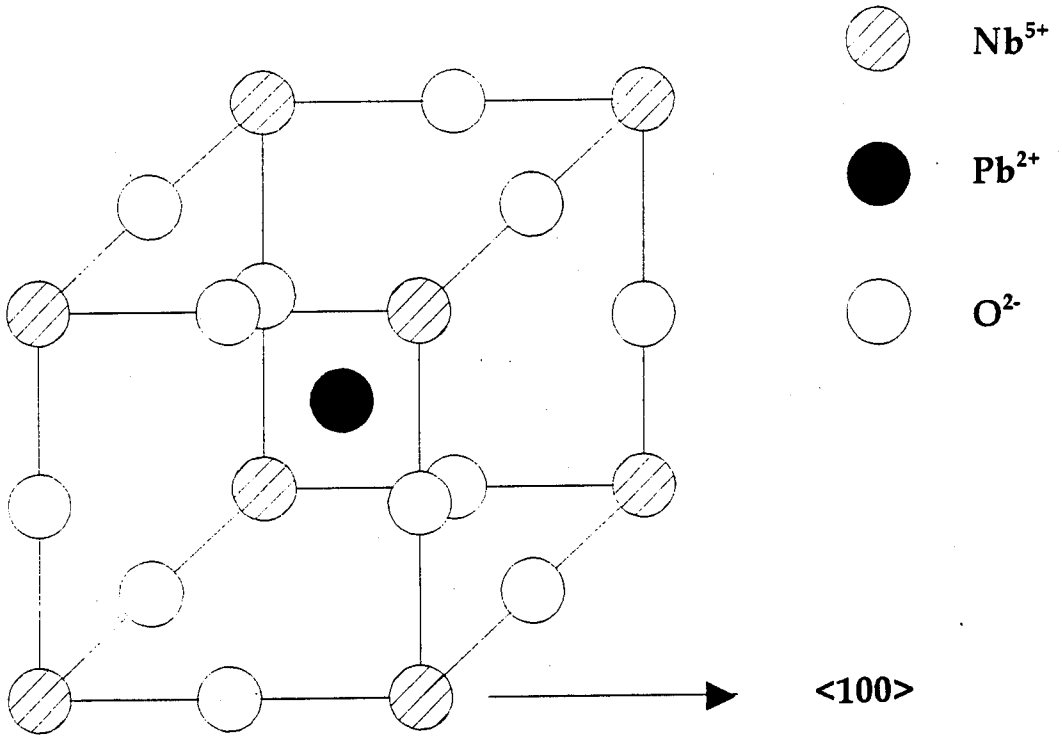

Figure 2. Unit Cell Crystal Structure of $PbNbO_3^{1+}$

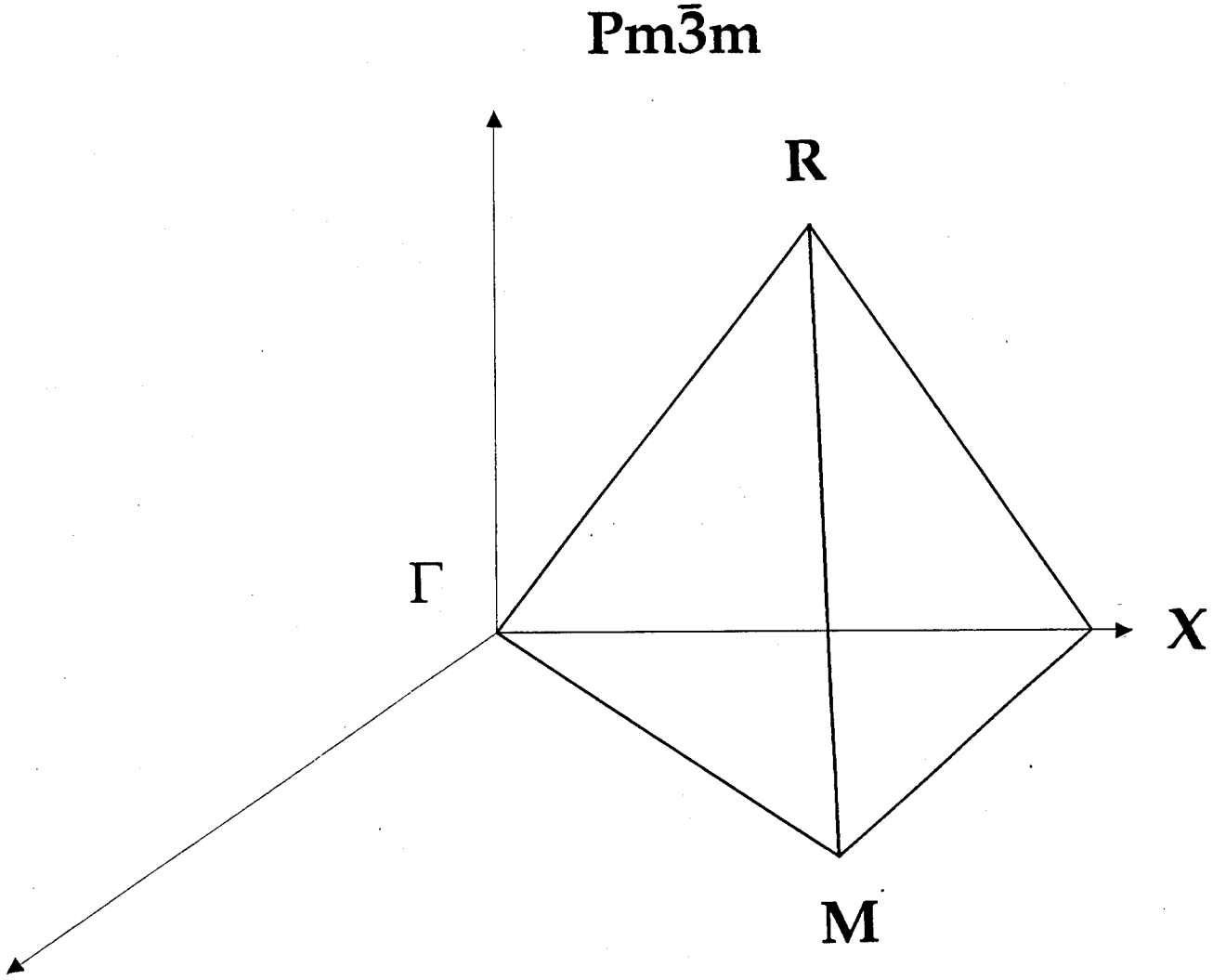

Figure 3. The Brillouin Zones in the Cubic Lattice

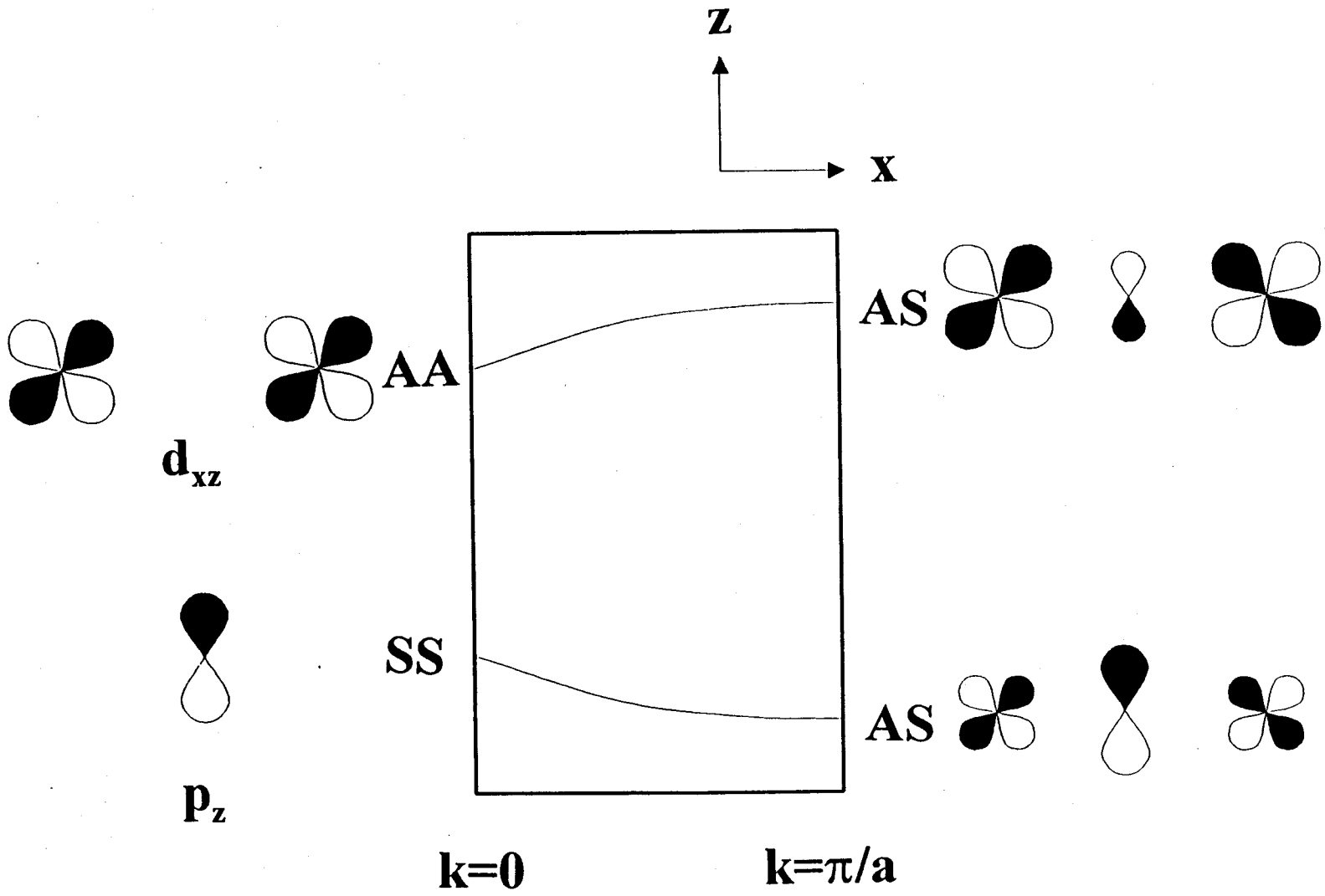

Figure 4. Band Energies of One-Dimensional Chain of Niobium and Oxygen Atoms

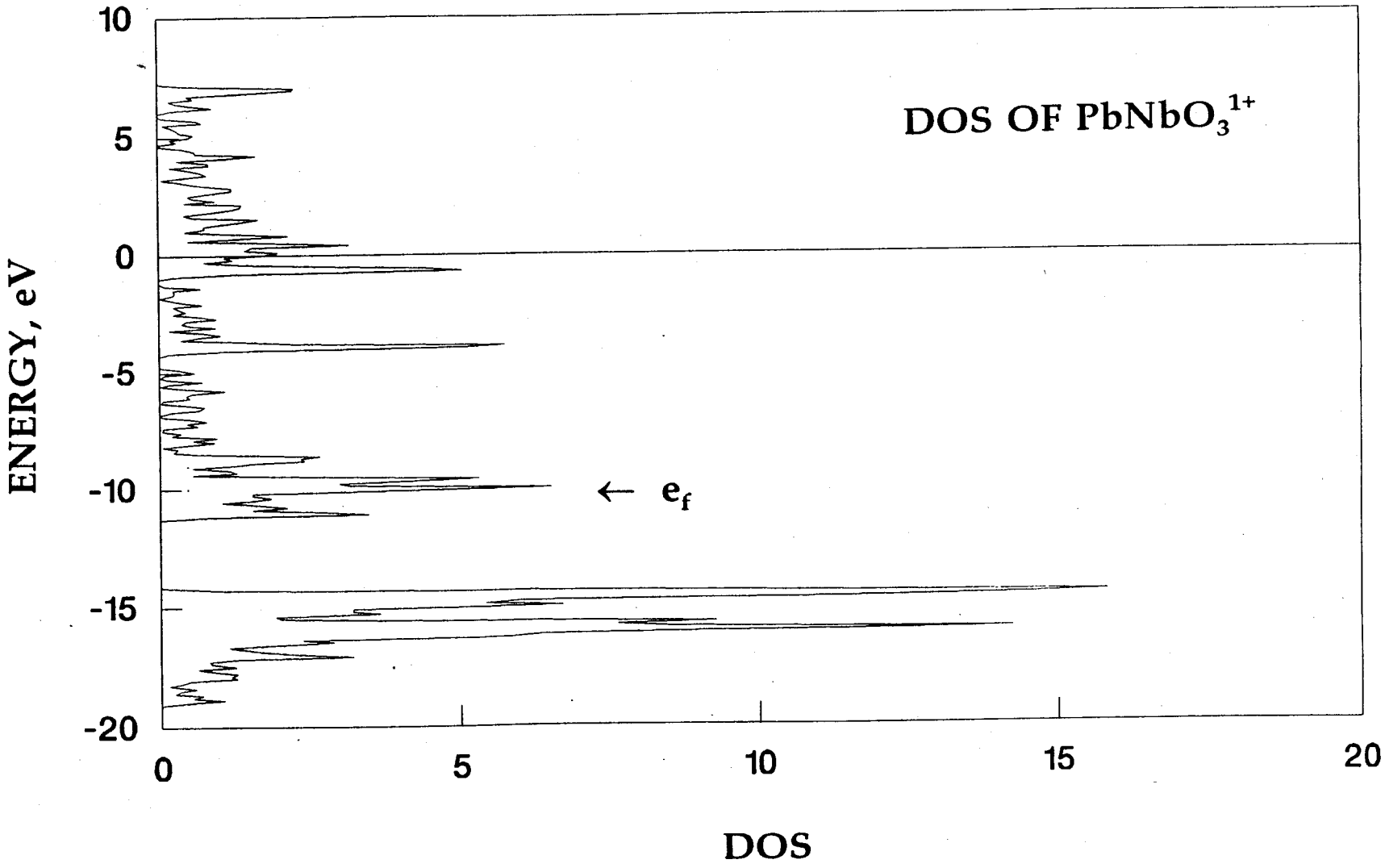

Figure 5. Density of States (DOS) of $PbNbO_3^{1+}$

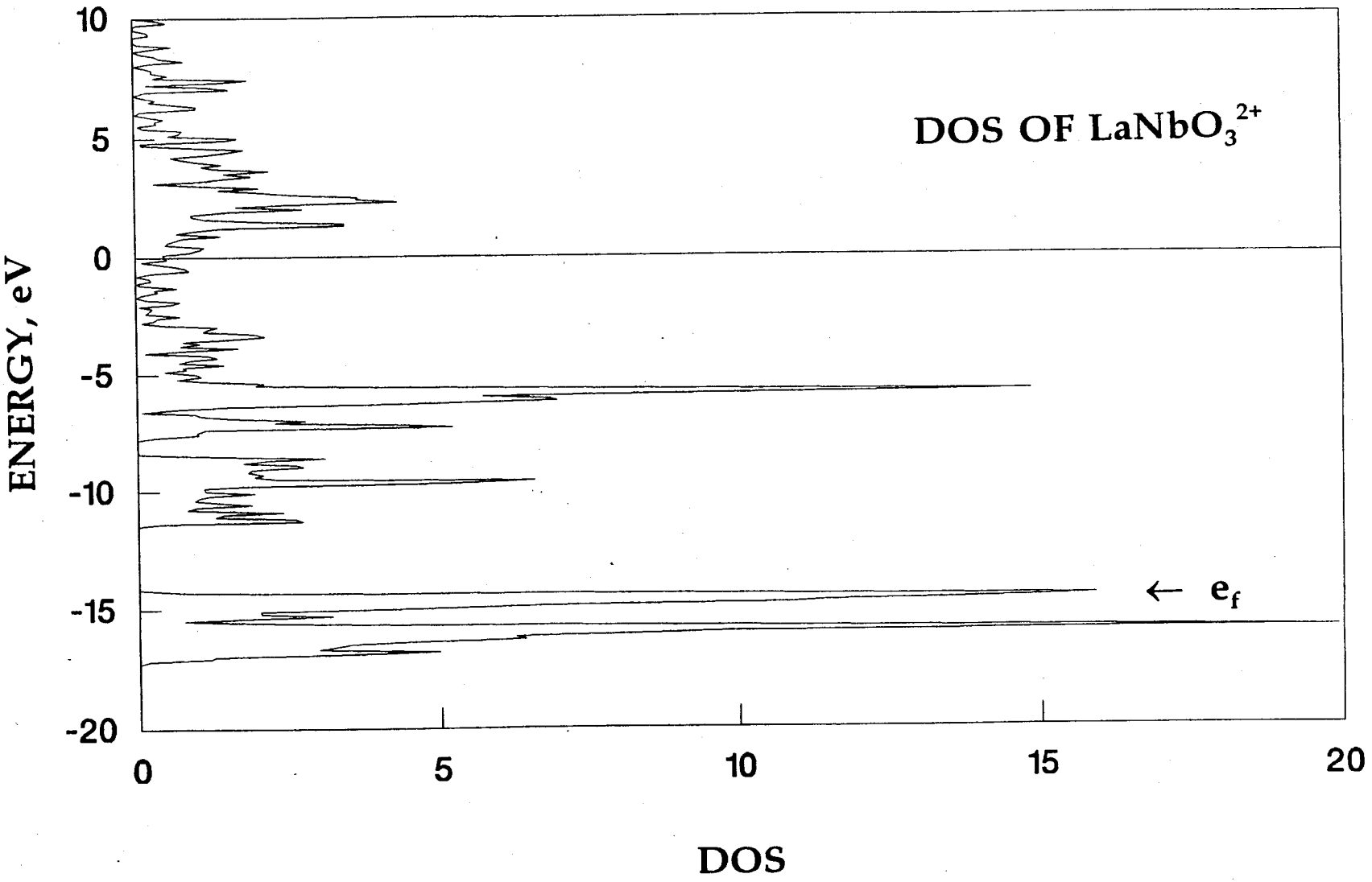

Figure 6. Density of States (DOS) of $LaNbO_3^{2+}$

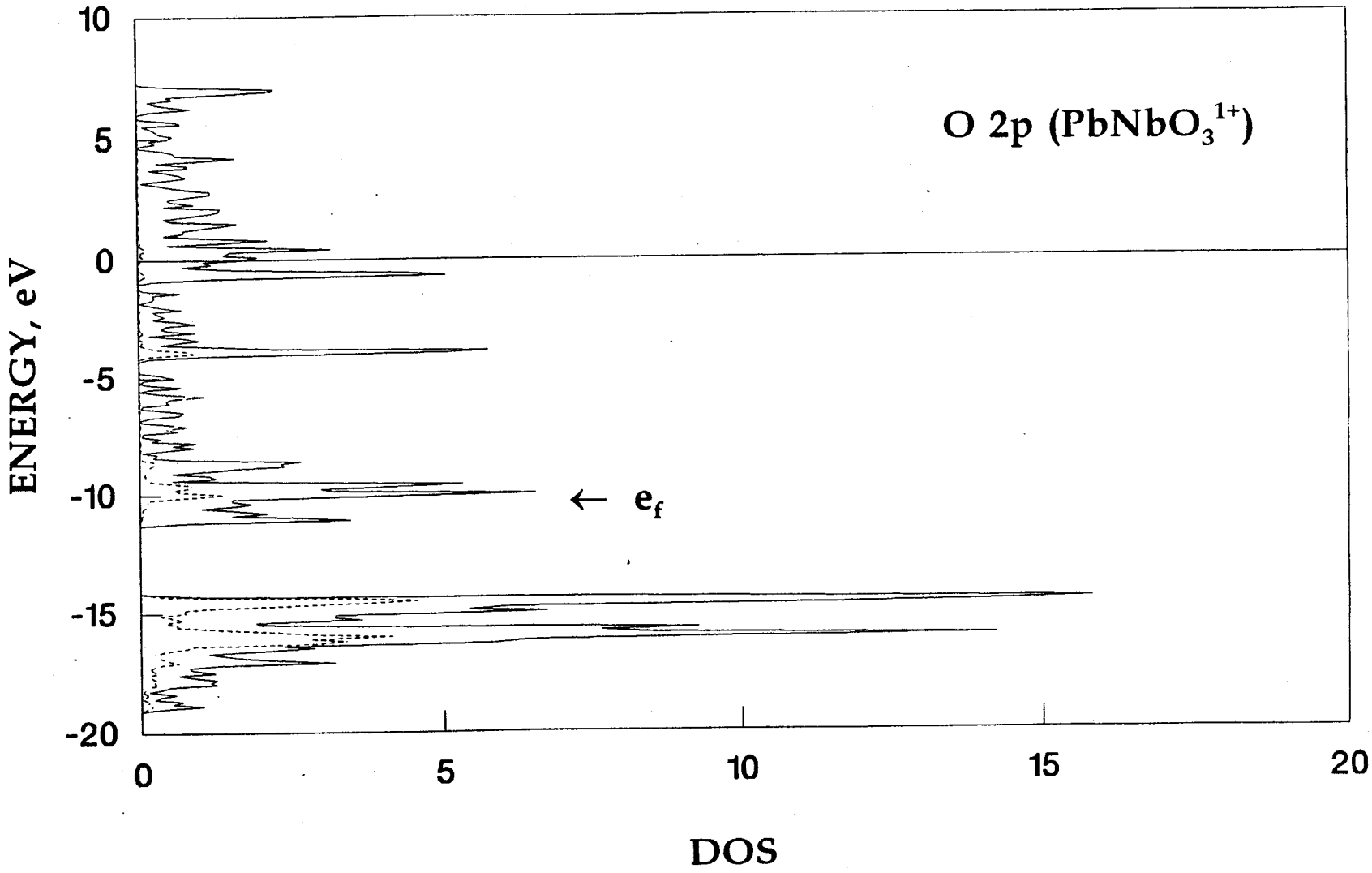

Figure 7. Contribution of Oxygen 2p Bands to DOS in $PbNbO_3^{1+}$

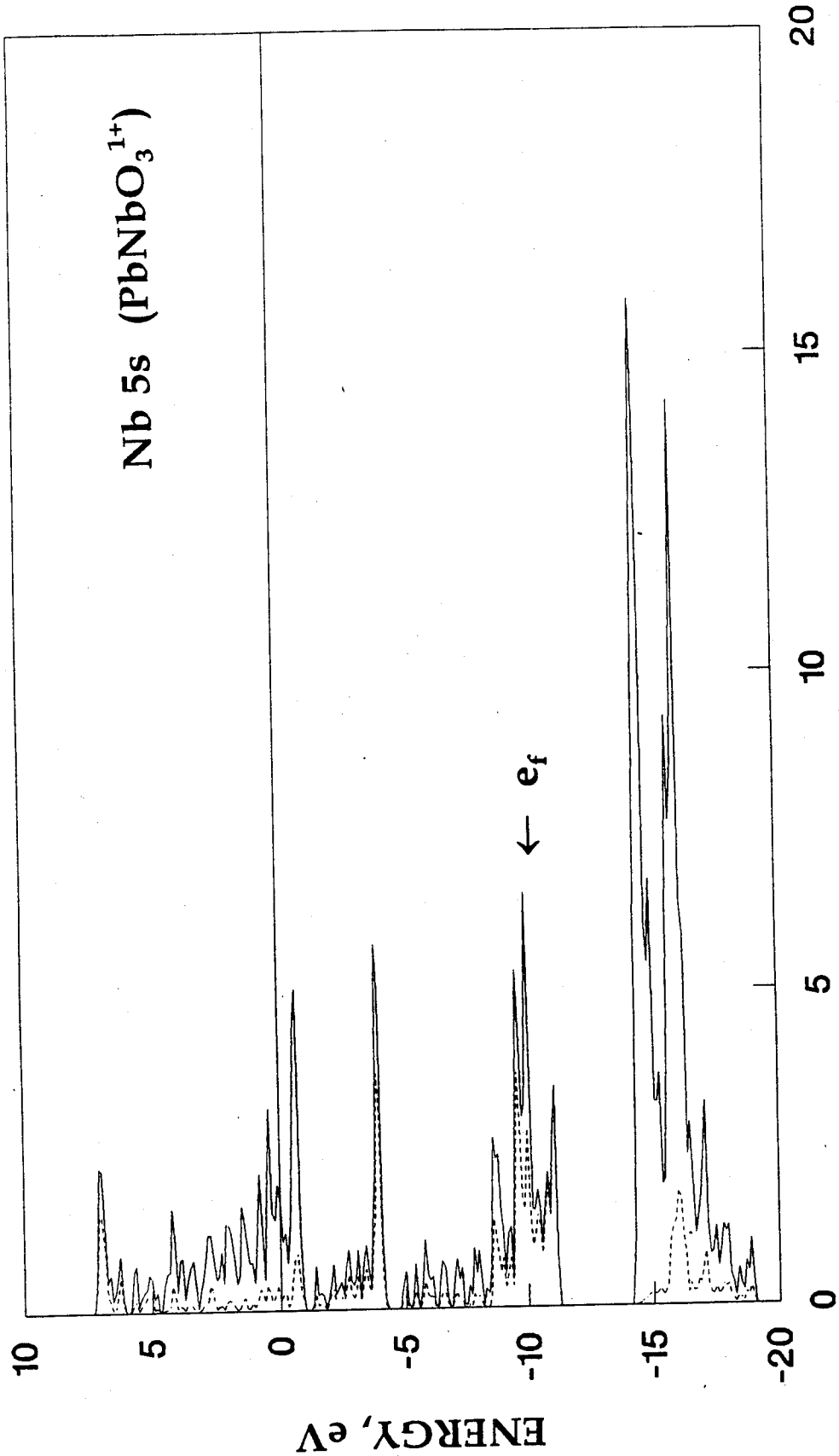

Figure 8. Contribution of Niobium 5s Bands to DOS in $PbNbO_3^{1+}$

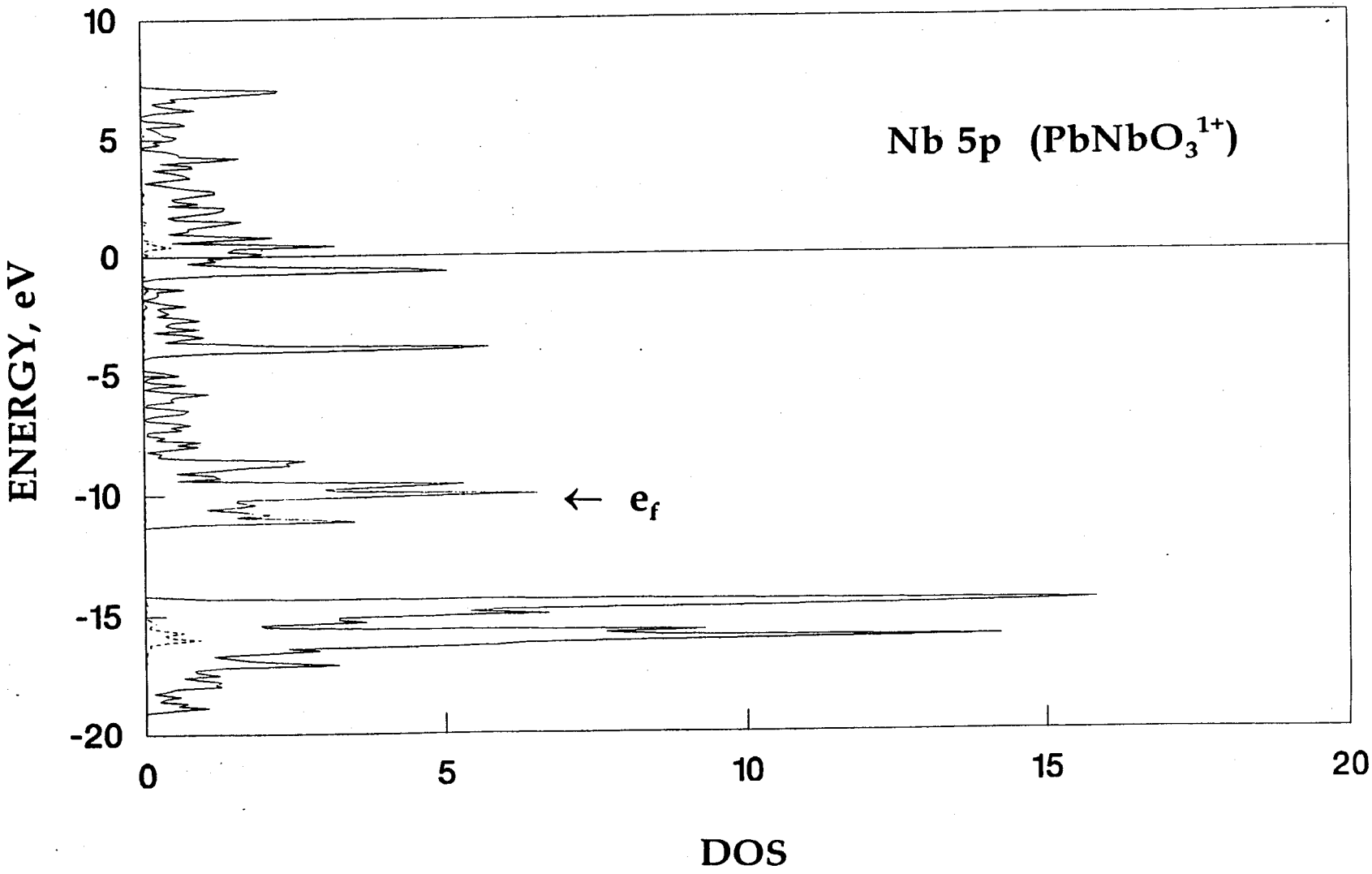

Figure 9. Contribution of Niobium 5p Bands to DOS in $PbNbO_3^{1+}$

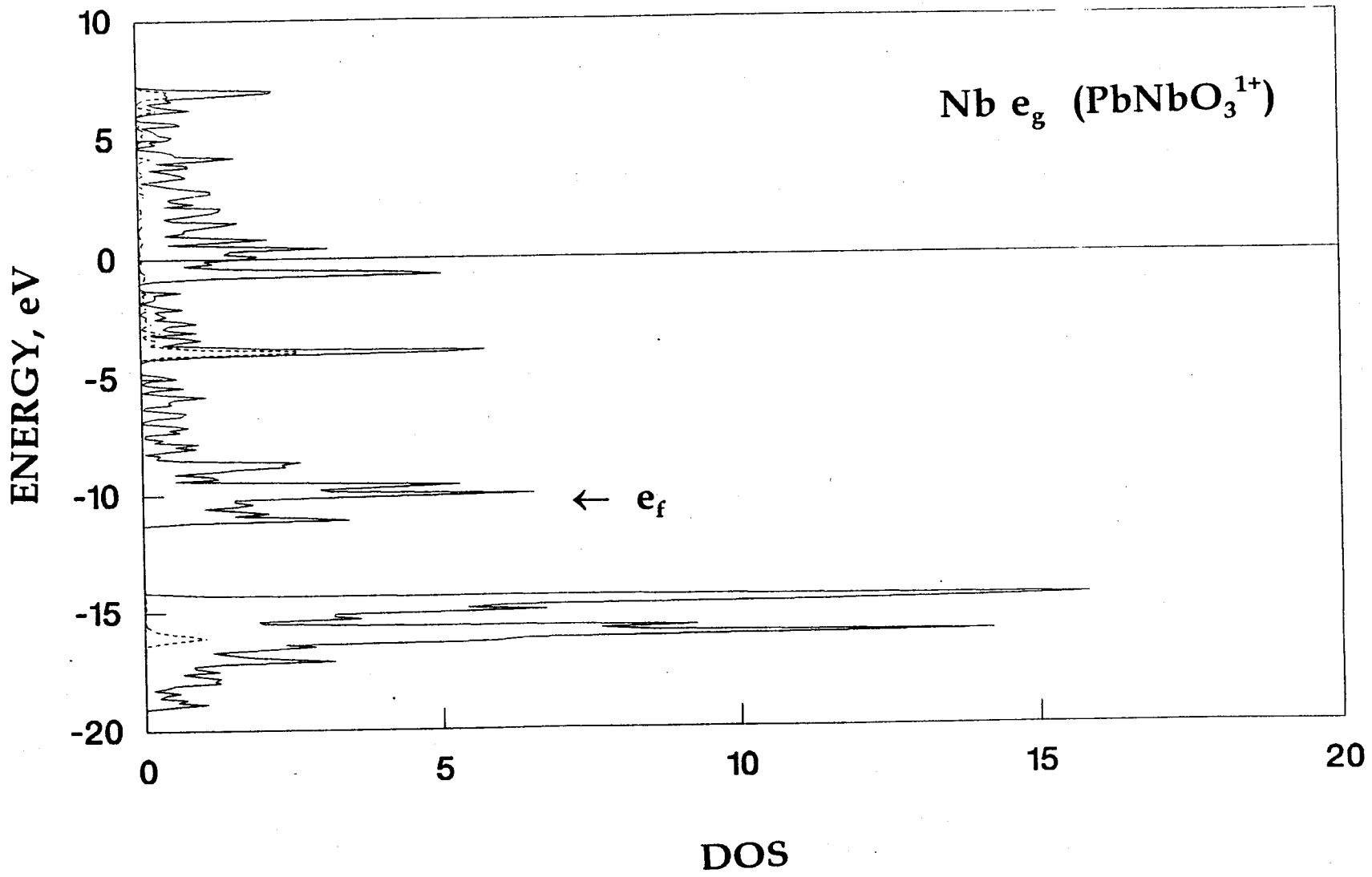

Figure 10. Contribution of Niobium e_g Bands to DOS in $PbNbO_3^{1+}$

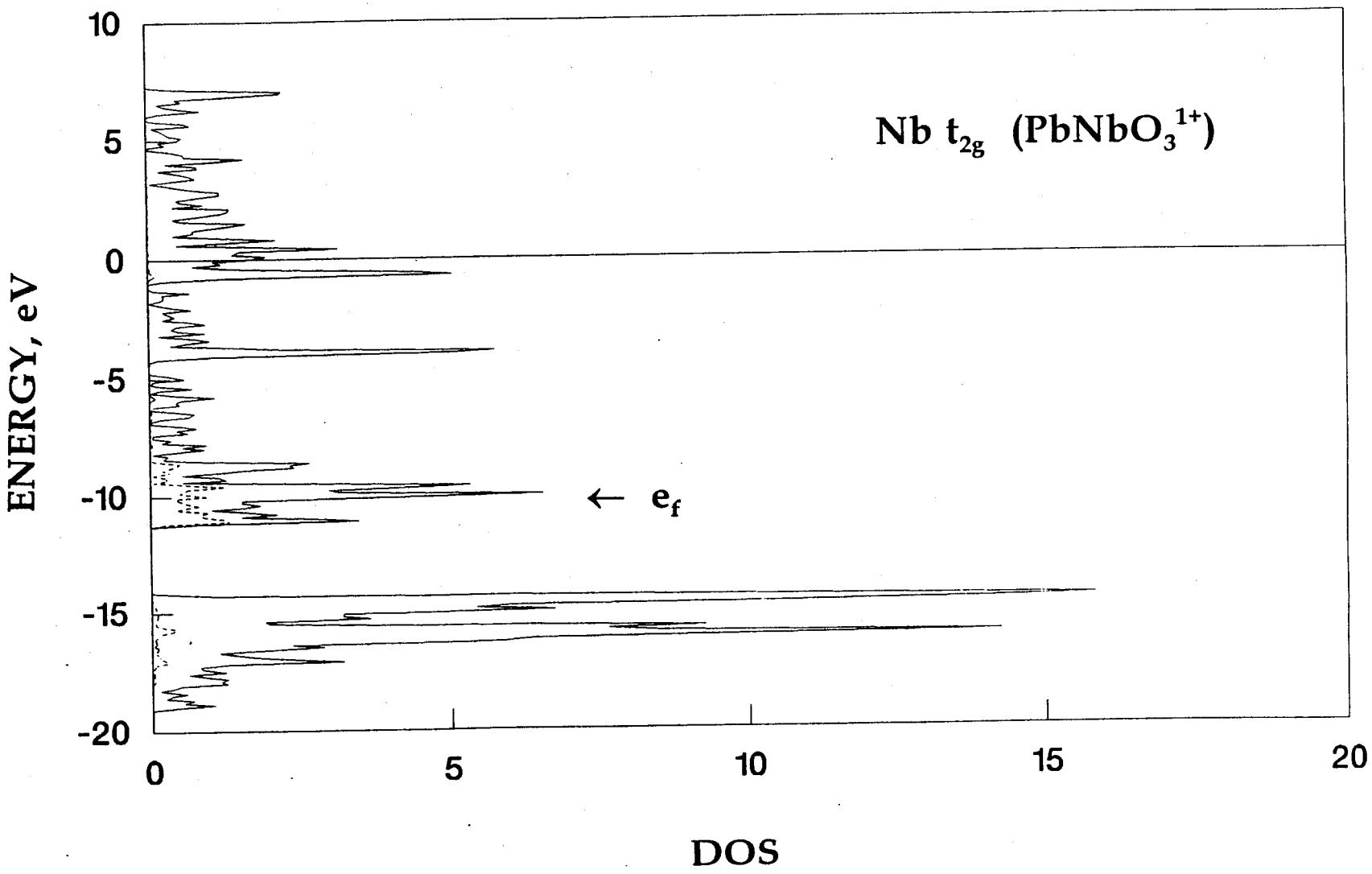

Figure 11. Contribution of Niobium t_{2g} Bands to DOS in $PbNbO_3^{1+}$

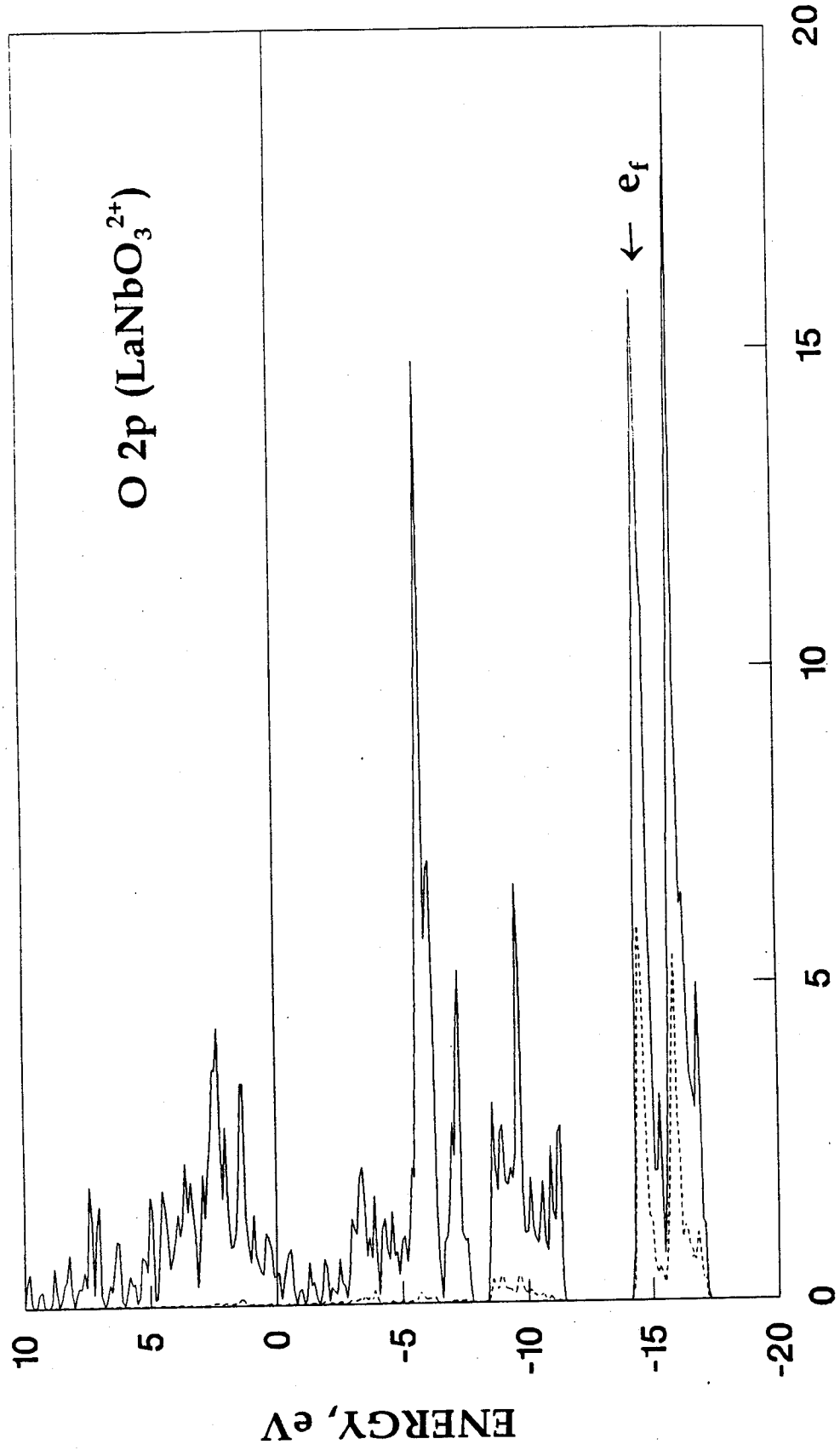

Figure 12. Contribution of Oxygen 2p Bands to DOS in $LaNbO_3^{2+}$

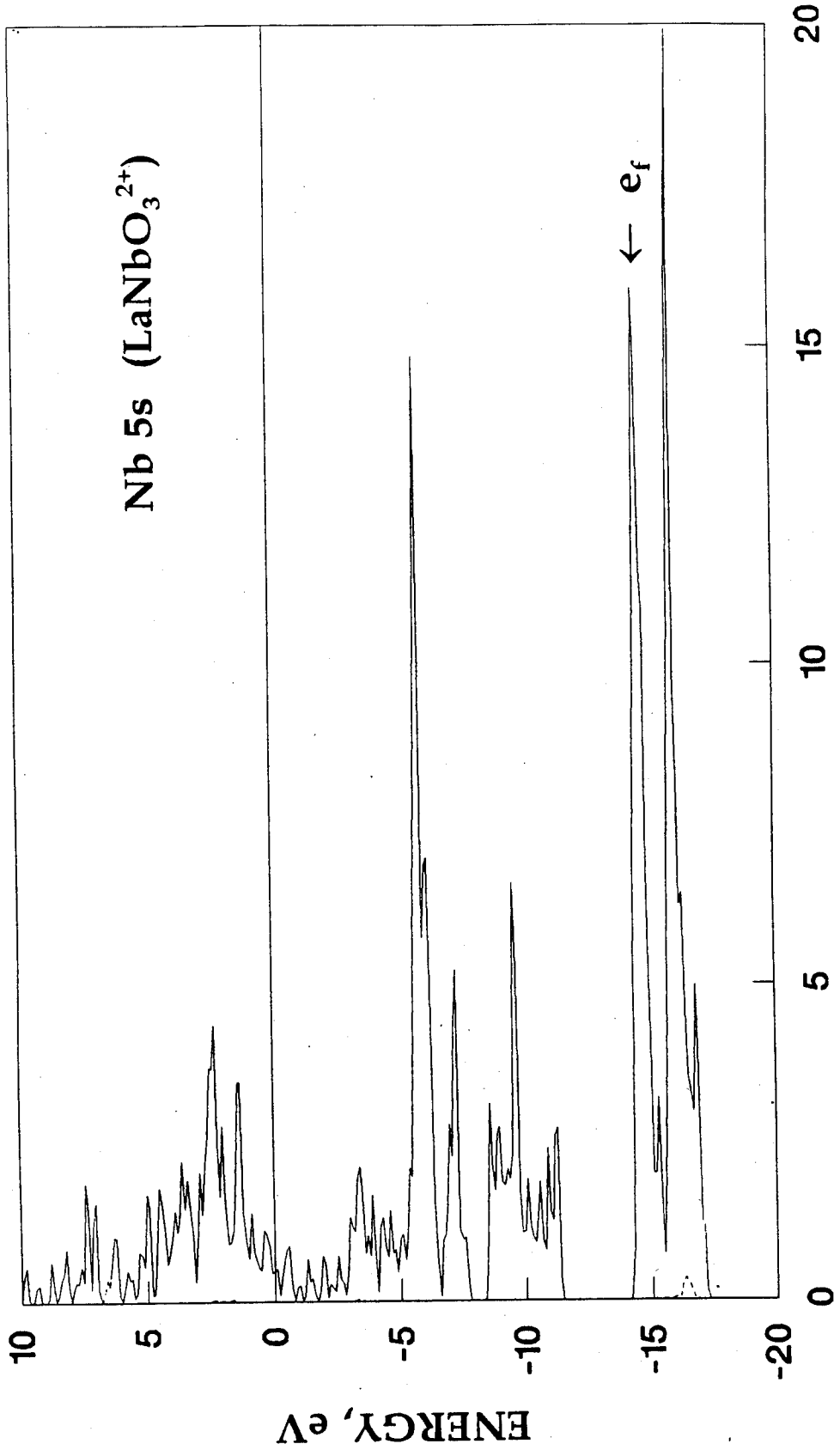

Figure 13. Contribution of Niobium 5s Bands to DOS in $LaNbO_3^{2+}$

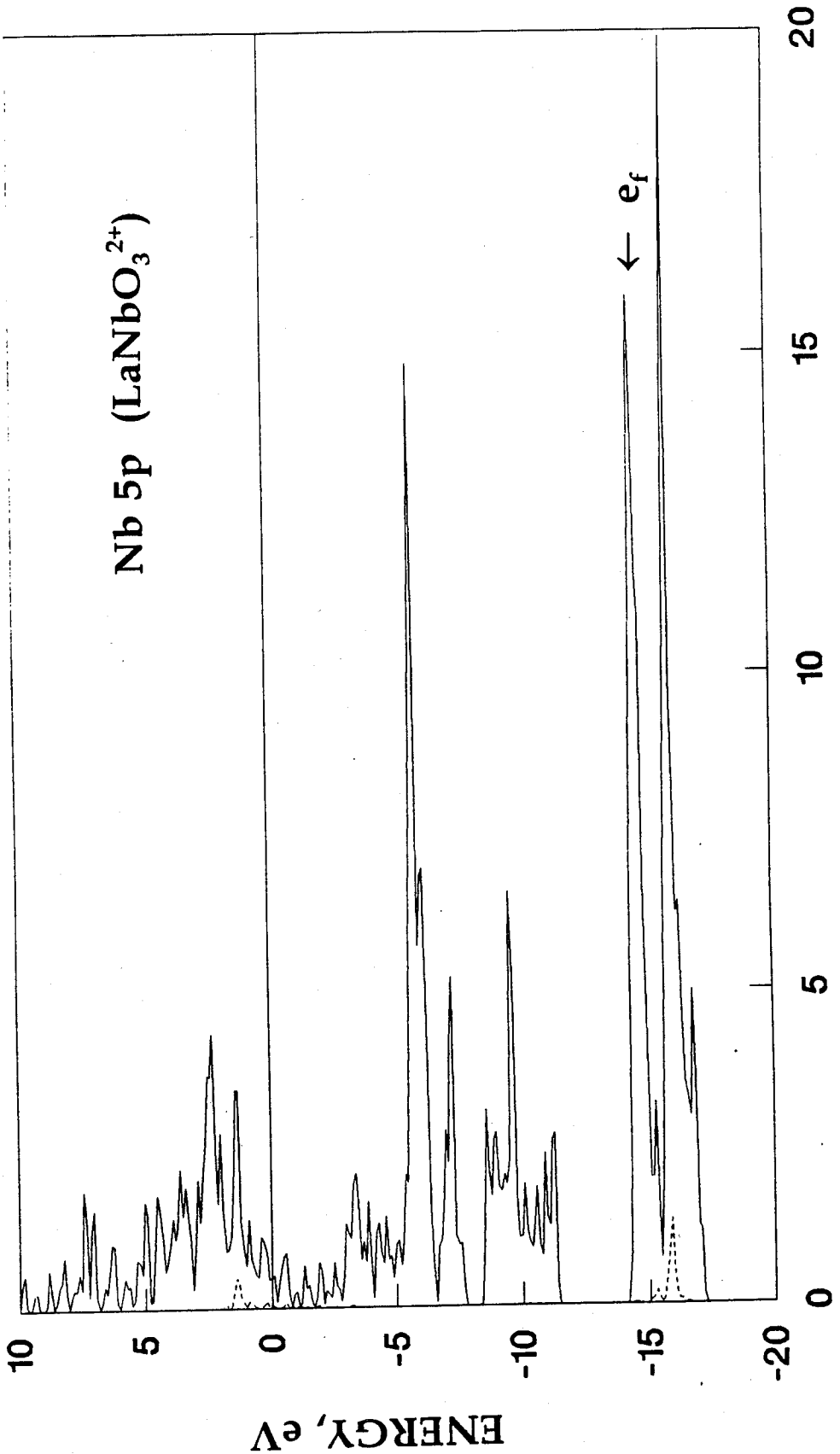

Figure 14. Contribution of Niobium 5p Bands to DOS in $LaNbO_3^{2+}$

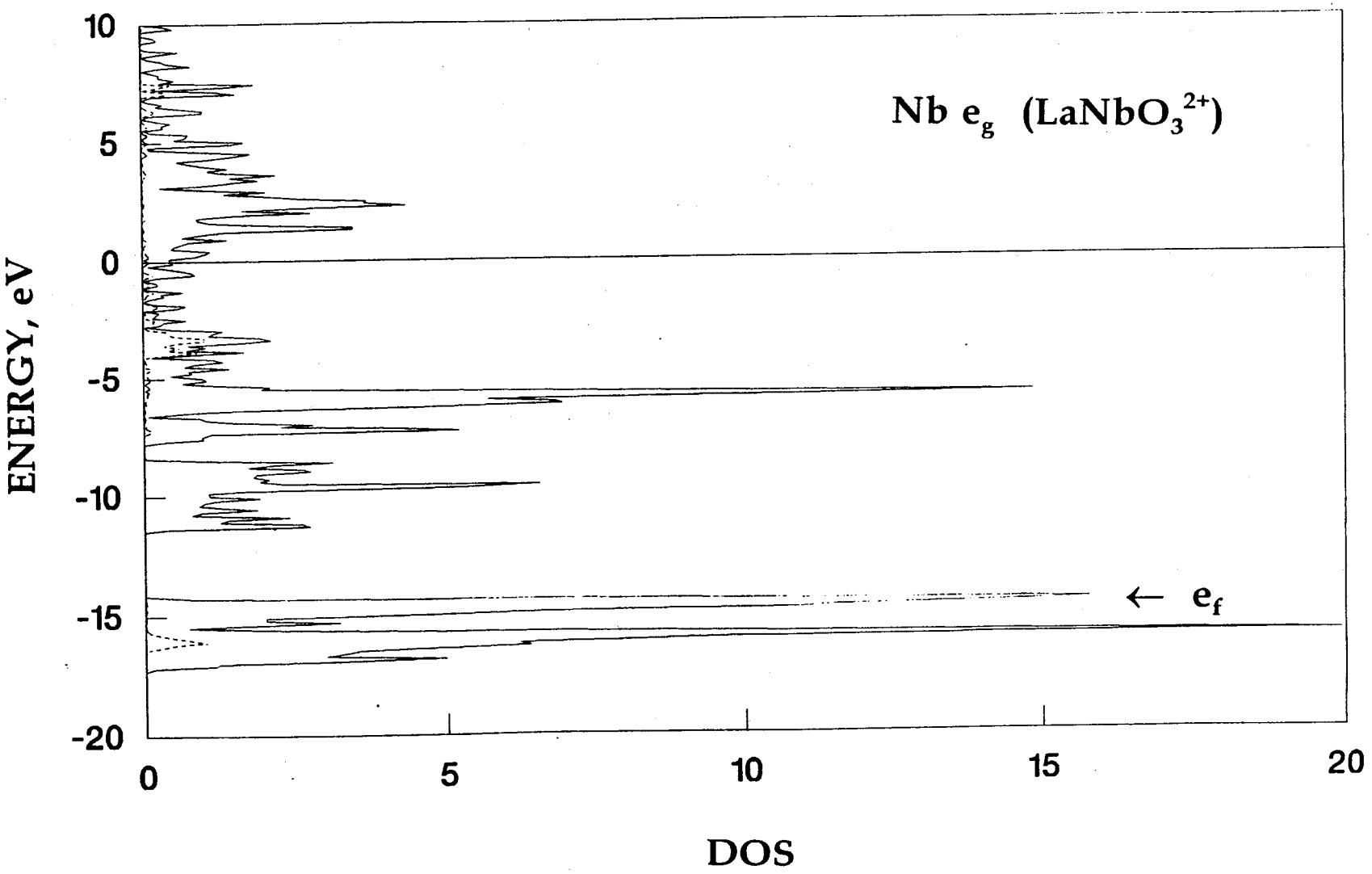

Figure 15. Contribution of Niobium e_g Bands to DOS in $LaNbO_3^{2+}$

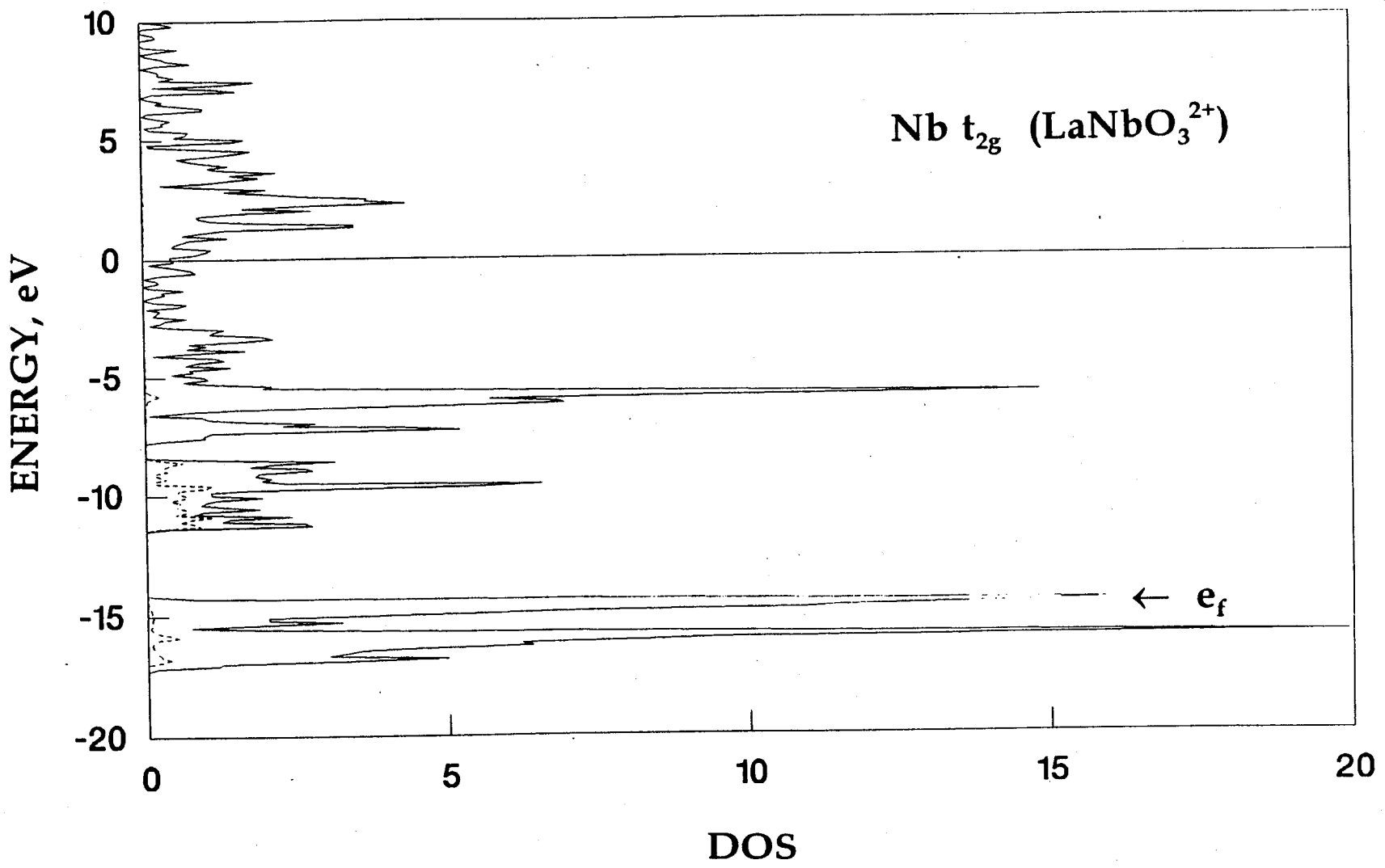

Figure 16. Contribution of Niobium t_{2g} Bands to DOS in $LaNbO_3^{2+}$

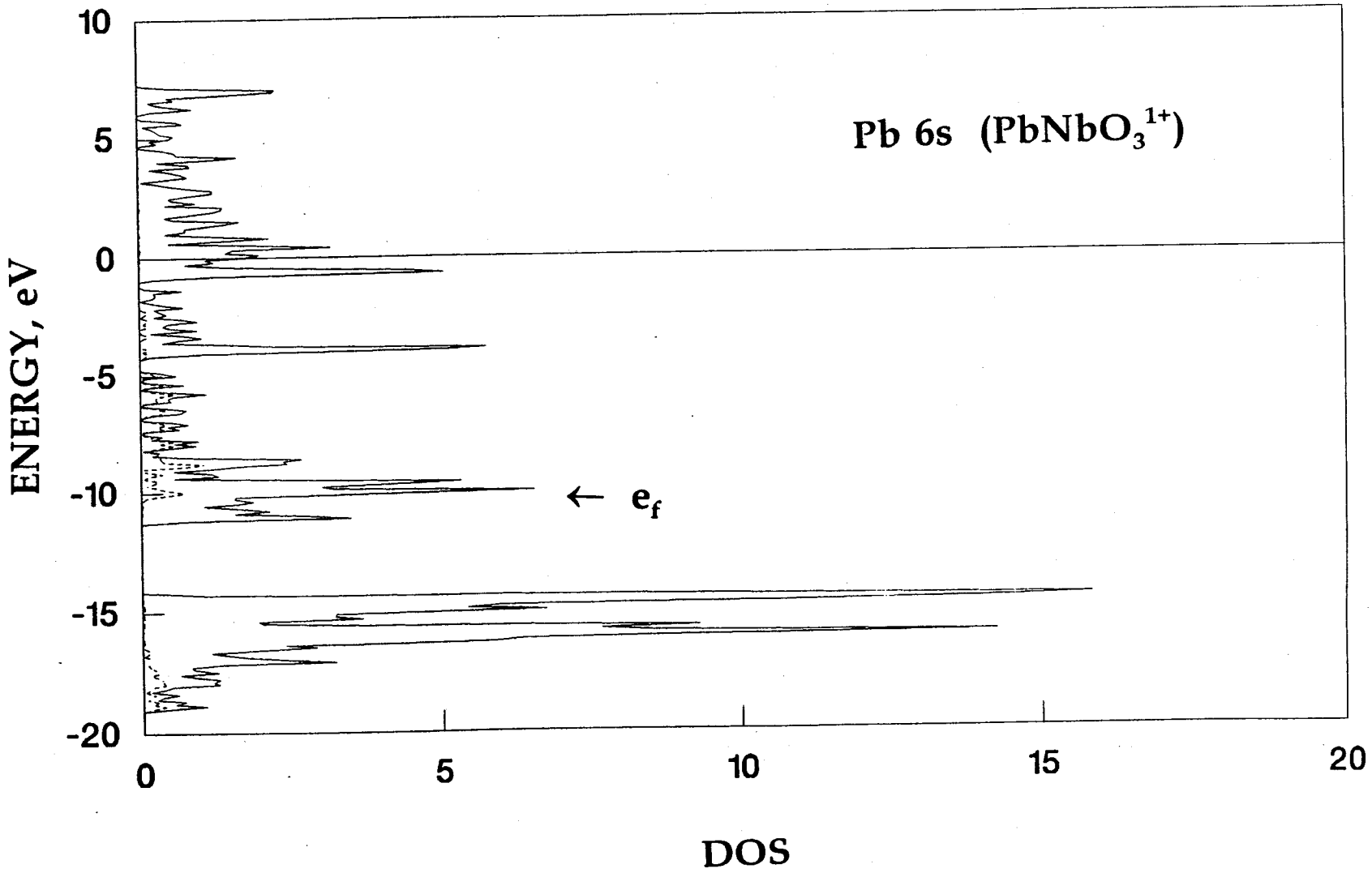

Figure 17. Contribution of Lead 6s Bands to DOS in $PbNbO_3^{1+}$

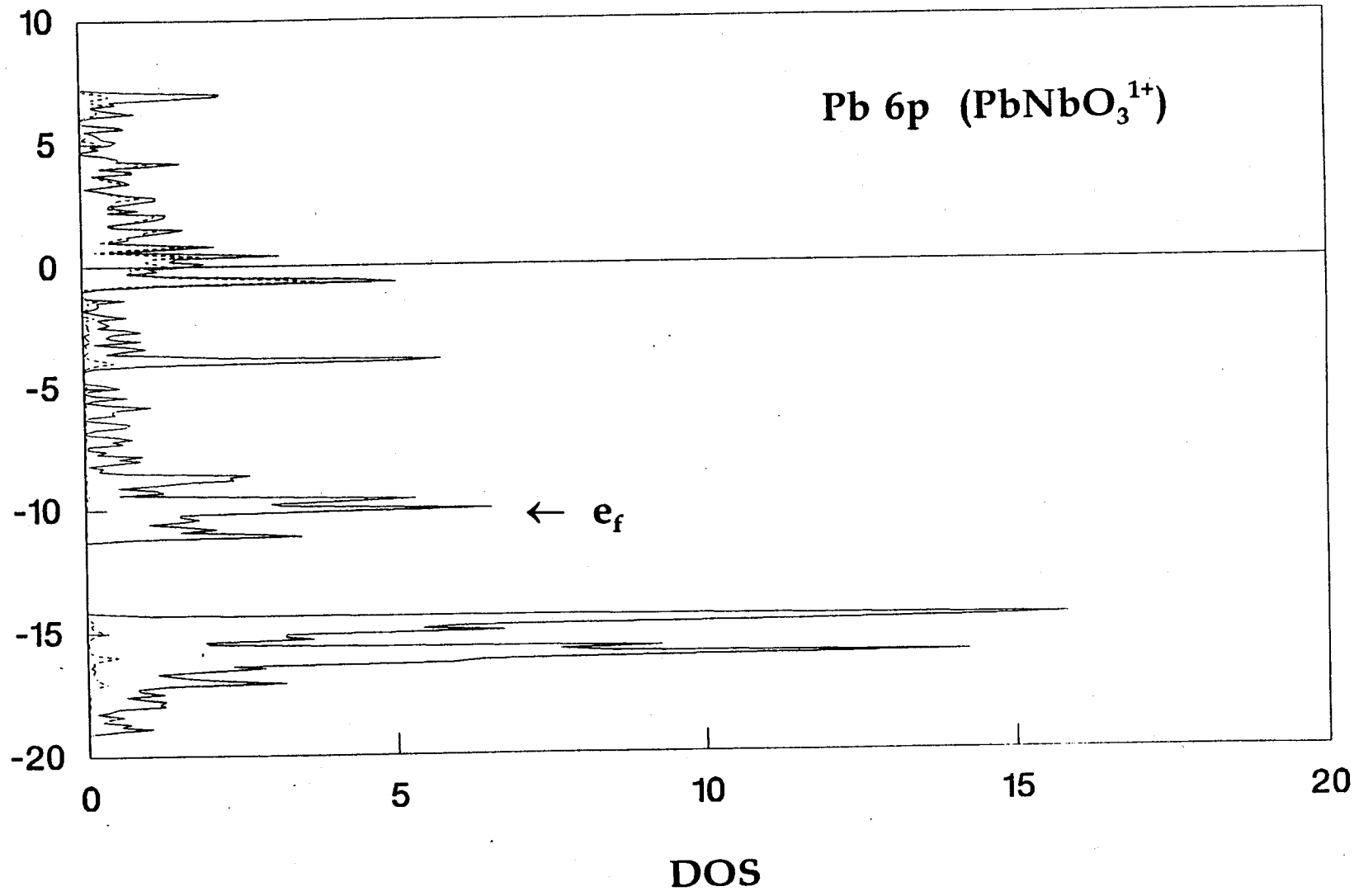

Figure 18. Contribution of Lead 6p Bands to DOS in $PbNbO_3^{1+}$

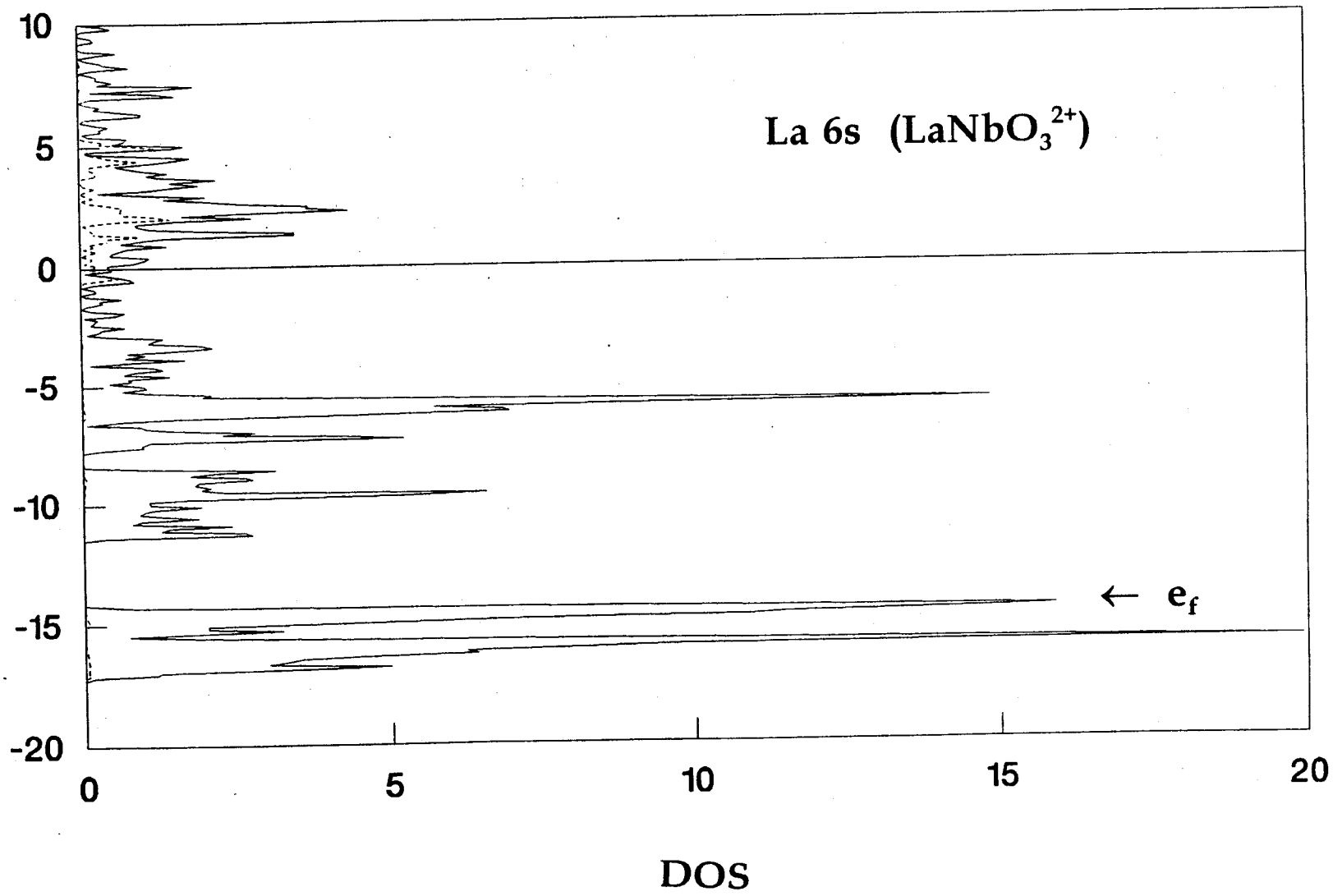

Figure 19. Contribution of Lanthanum 6s Bands to DOS in $LaNbO_3^{2+}$

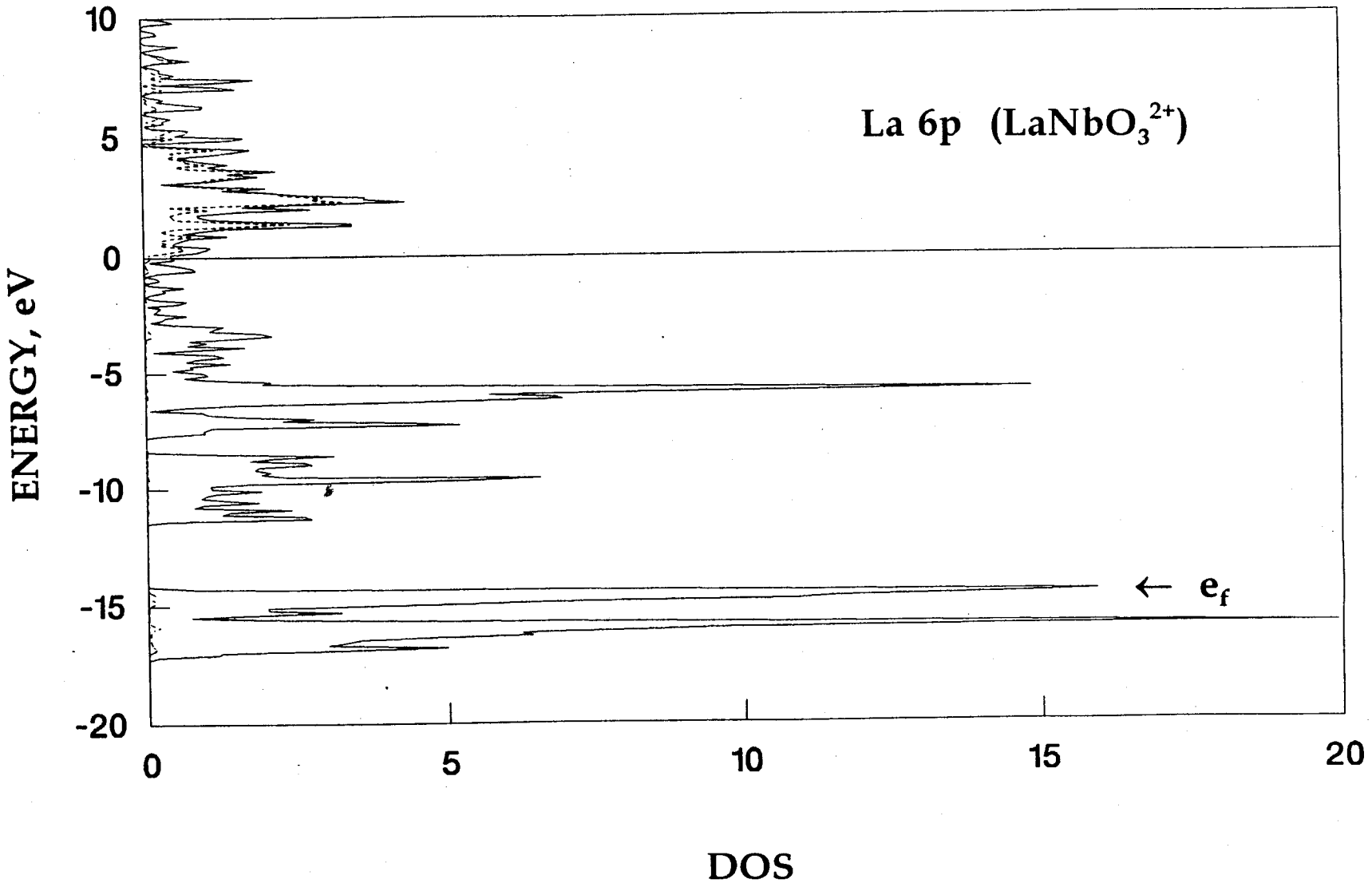

Figure 20. Contribution of Lanthanum 6p Bands to DOS in $LaNbO_3^{2+}$

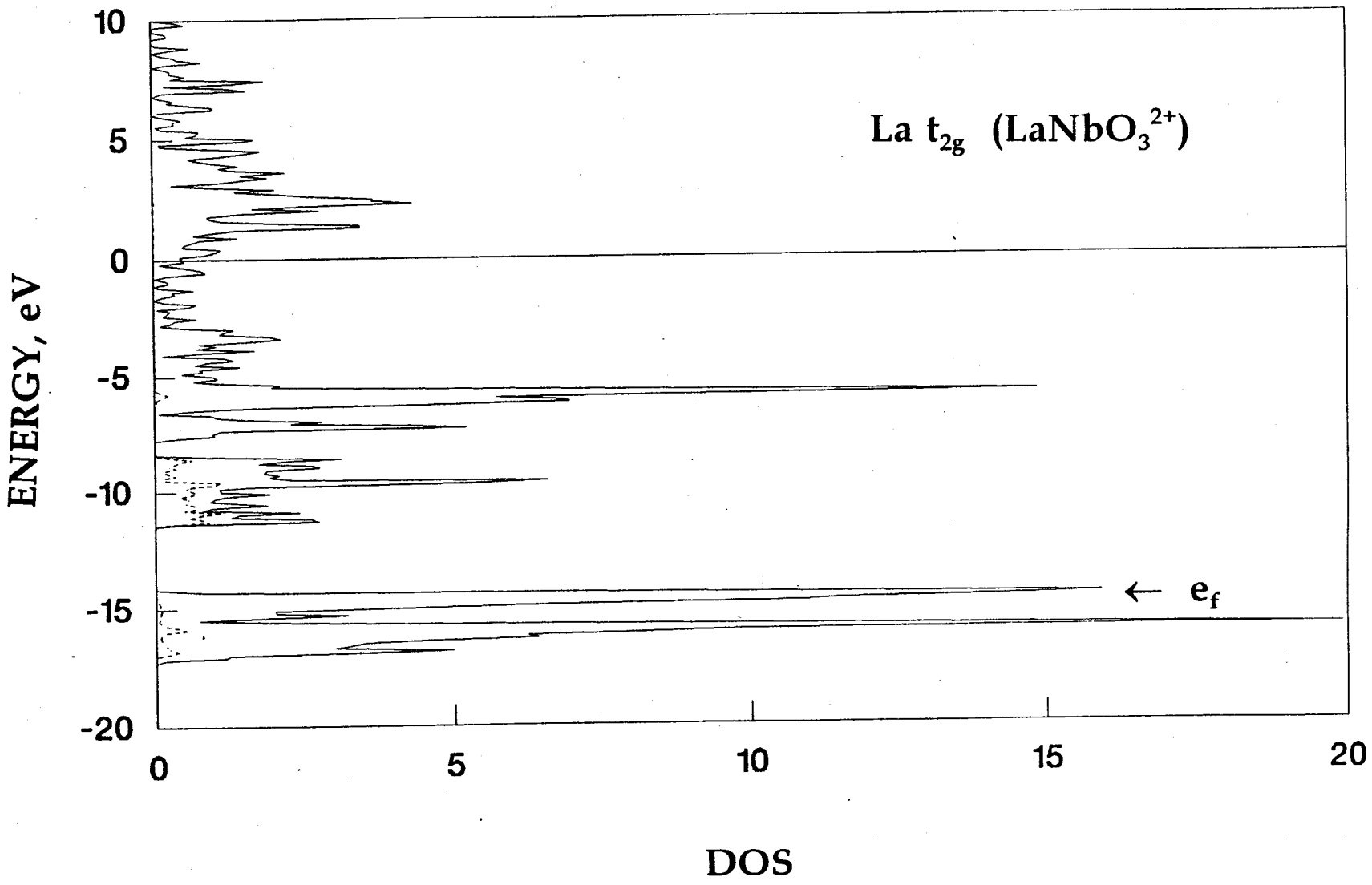

Figure 21. Contribution of Lanthanum t_{2g} Bands to DOS in $LaNbO_3^{2+}$

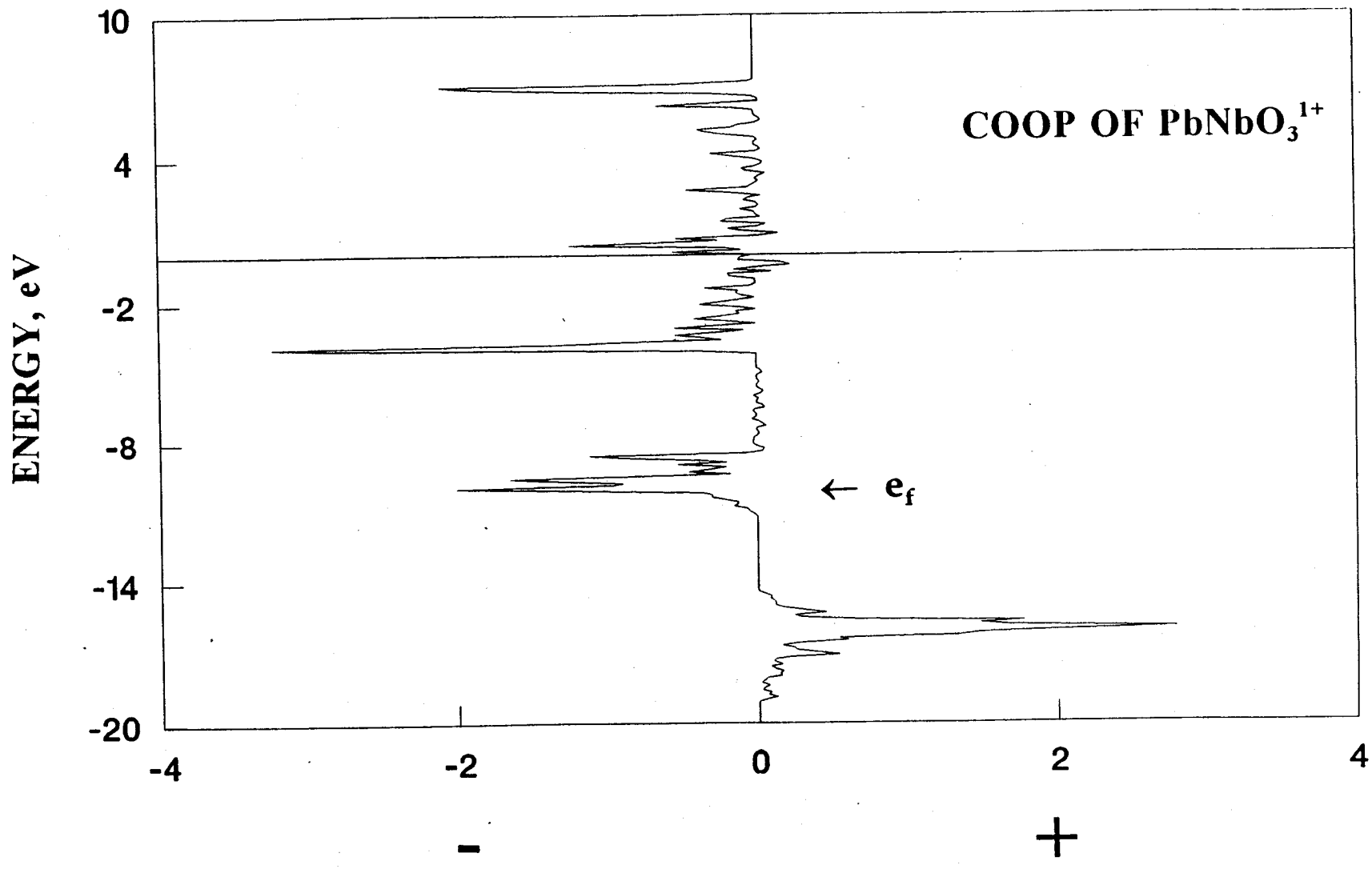

Figure 22. Crystal Orbital Overlap Population (COOP) in $PbNbO_3^{1+}$

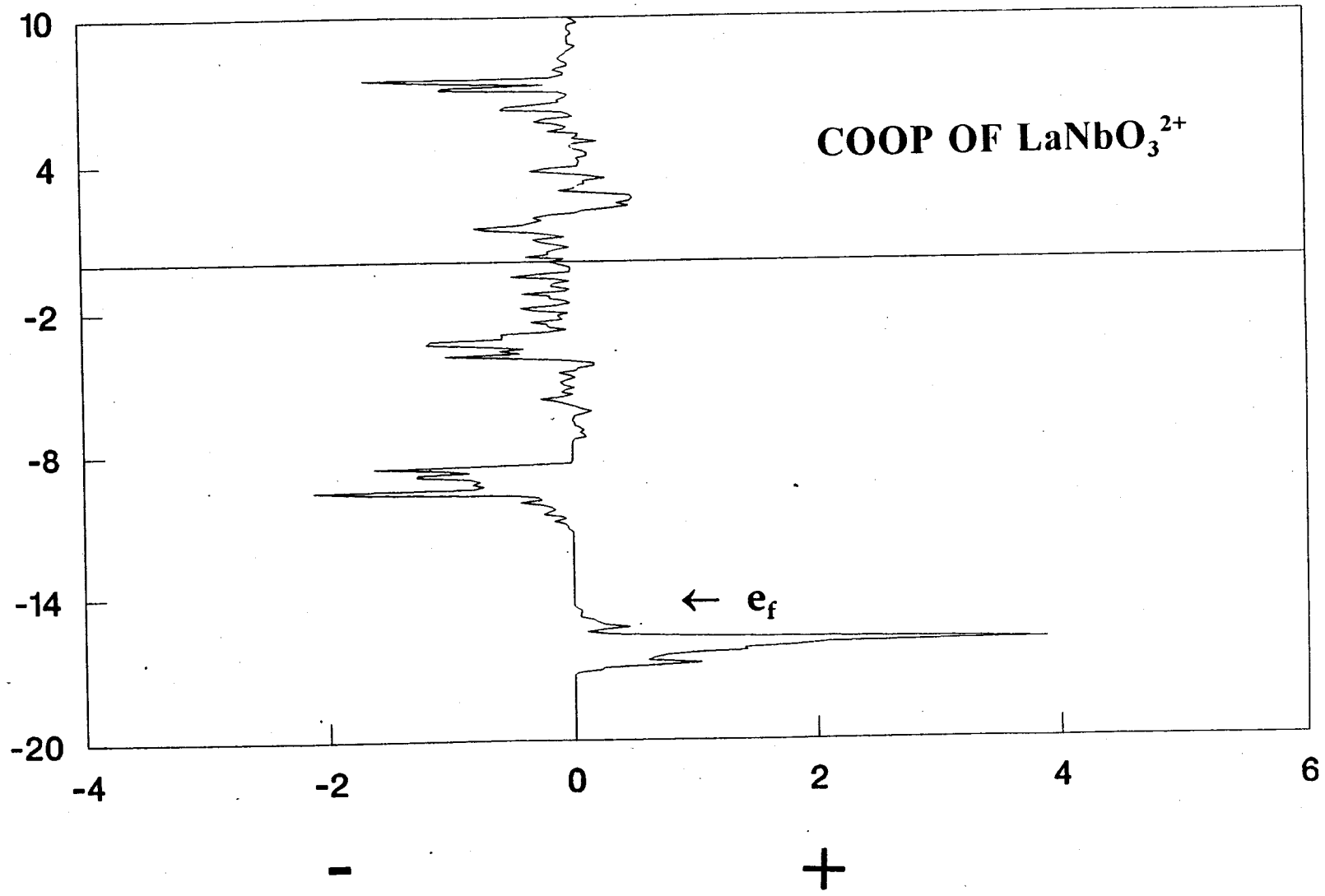

Figure 23. Crystal Orbital Overlap Population (COOP) in $LaNbO_3^{2+}$

Table 1. Extended Hückel Parameters[a]

atom	orbital	H_{ii} eV	ζ_1[b]	ζ_2[b]	c_1	c_2
Nb	5s	-10.1	1.89	-	1.0000	-
	5p	-6.86	1.85	-	1.0000	-
	4d	-12.1	4.08	1.64	0.6401	0.55160
Pb	6s	-15.7	2.35	-	1.0000	-
	6p	-8.0	2.06	-	1.0000	-
La	6s	-7.67	2.14	-	1.0000	-
	6p	-5.01	2.08	-	1.0000	
	5d	-8.21	3.78	1.381	0.77651	0.45861
O	2s	-32.3	2.275	-	1.0000	-
	2p	-14.8	2.275	-	1.0000	-

[a]M.-H. Whangbo, M. Evain, T. Hughbanks, M. Kertesz, S. Wijeyesekera, C. Wilker, C. Zheng, and R. Hoffmann, "Extended Hückel Molecular, Crystal and Properties Package," QCPE 571 Program, Quantum Chemistry Program Exchange, Indiana University.

[b]Slater exponents.

Table 2. Electronic Configurations[a]

atom	electronic configuration
Nb	$4d^4 5s^1$
Pb	$5d^{10} 6s^2 6p^2$
La	$5d^1 6s^2$
O	$2s^2 2p^4$

[a]Outer orbitals only.

REFERENCES

1. L. E. Cross, "Relaxor Ferroelectrics," *Ferroelectrics*, vol. 76, 1987, p. 241.

2. D. Viehland, M. Wuttig, and L. E. Cross, "Internal Strain and Anelastic Relaxations in Lead Magnesium Niobate," *Philosophical Magazine*, vol. A 64, 1991, p. 835.

3. D. Viehland, J. F. Li, M. Wuttig, and L. E. Cross, "The Glassy Polarization Behavior of Relaxor Ferroelectrics," *Physics Reviews*, vol. B46, 1992, p. 8013.

4. C. Randall, D. Barber, and R. Whatmore, "A TEM Study of Ordering in the Perovskite, $Pb(Sc_{1/2}Ta_{1/2})O$," *Journal of Material Science*, vol. 21, 1986, p. 4456.

5. D. Viehland and J. Li, "Compositional Instability and the Resultant Charge Variations in Mixed B-Site Cation Relaxor Ferroelectrics," *Journal of Applied Physics*, vol. 74, 1993, p. 4121.

6. K. Park, L. Salamanca-Riba, M. Wuttig, and D. Viehland, "Ordering in Lead Magnesium Niobate Solid Solutions," *Journal of Materials Science*, vol. 29, 1994, p. 1284.

7. J. Chen, H. M. Chan, and M. P. Harmer, "Ordering Structure and Dielectric Properties of Undoped and La/Na-Doped $Pb(Mg_{1/3}Nb_{2/3})O_3$," *Journal of the American Ceramic Society*, vol. 72, 1989, p. 593.

8. N. W. Thomas, "A New Framework for Understanding Relaxor Ferroelectrics," *Journal of Physics and Chemistry of Solids*," vol. 51, 1990, p. 1419.

9. Z.-K. Xu and D. Viehland, "The Nonuniform Ordered Structure of Perovskite Lead Magnesium Niobate," submitted.

10. S. M. Pilgrim, M. Massuda, and A. E. Sutherland, "Electromechanical Determination of the High-Field Phase Transition of $Pb(Mg_{1/3}Nb_{2/3})O_3$-$PbTiO_3$-$(Ba,Sr)TiO_3$ Relaxor Ferroelectrics," *Journal of the American Ceramic Society*, vol. 75, 1992, p. 1970.

11. T. R. Shrout, W. Huebner, C. A. Randall, and A. D. Hilton, "Aging Mechanisms In $Pb(Mg_{1/3}Nb_{2/3})O_3$-Based Relaxor Ferroelectrics," *Ferroelectrics*, vol. 93, 1989, p. 361.

12. R. Hoffmann, *Solids and Surfaces: A Chemist's View of Bonding in Extended Structures*, VCH, New York, 1988.

13. E. Canadell and M.-H. Whangbo, "Conceptual Aspects of Structure-Property Correlations and Electronic Instabilities, with Applications to Low-Dimensional Transition-Metal Oxides," *Chemical Reviews*, vol. 91, 1991, p. 965.

14. C. R. A. Catlow in "Defects in Solids: Modern Techniques," ed. A. V. Chadwick and M. Terenzi (NATO ASI Series B: Physics vol. 147), Plenum, 1987.

15. G. J. Kavarnos, "Molecular Modeling: An Approach for the Study of Piezoelectric Polymers," NUWC-NPT Technical Report 10,771, Naval Undersea Warfare Center Detachment, New London, CT, 12 December 1994 (UNCLASSIFIED).

16. J. K. Burdett and T. Hughbanks, *J. Am. Chem. Soc.* **1984**, *106*, 3101.

17. V. A. Pokov and I. E. Mylinkova, "Electrical and Optical Properties of Simple Crystals of Ferroelectrics with a Diffused Phase Transition," *Soviet Physics - Solid State (English Transition)*, vol. 3, 1961, p. 613.

18. I. G. Ismailzade, "An X-ray Study of the $Pb_3NiNb_2O_9$-$Pb_3MgNb_2O_9$ System," *Soviet Physics - Crystallography (English Translation)*, vol. 5, 1960, p. 292.

19. R. Ramirez and M. C. Böhm, "The Use of Symmetry In Reciprocal Space Integrations. Asymmetric Units and Weighting Factors for Numerical Integration Procedures in any crystal Symmetry," *International Journal of Quantum Chemistry*, vol. XXXIV, 1988, p. 571.

INITIAL DISTRIBUTION LIST

Addressee	No. of Copies
Office of Naval Research (Dr. W. A. Smith, Code 332; Dr. K. J. Wynne, Code 1113)	2
Pennsylvania State University (Prof. L. E. Cross, Prof. Q. Zhang, Prof. T. R. Shrout)	3
University of Illinois-Urbana (Prof. D. Viehland)	1
Defense Technical Information Center	2